XIV School on Synchrotron Radiation:
Fundamentals, Methods and Applications

Muggia, Italy / 18-29 September 2017

MAGNETIC AND RESONANT X-RAY DIFFRACTION

Luigi Paolasini
European Synchrotron Radiation Facility
paolasini@esrf.eu

OUTLINES

1. Magnetism and magnetic structures
2. Theory of x-ray magnetic and resonant scattering
3. Experimental methods: polarized x-rays
4. Non-resonant magnetic scattering
5. Resonant x-ray scattering and high order multipoles
6. Resonant inelastic scattering

Books:
- Jens Als-Nielsen and Des McMorrow , “Elements of Modern X-ray Physics”, Second edition, John Wiley & Sons, Ltd Publication, (2011).
- “Synchrotron Radiation: Basics, Methods and Applications”, Ed. Mobilio, Boschierini, Meneghini, Springer-Heidelberg 2015.

Articles:
- M. Blume,*”Resonant anomalous x-ray scattering”*, ed. G. Materlik, (1994), p. 494-512, Elsevier Science B.V., Amsterdam. *(Theory)*
- Paolasini and de Bergevin, CR Physique 9 550 (2008) *(nRMXS and REXS)*
- Di Matteo, J. Phys. D: Appl. Phys. 45 163001 (2012) *(REXS and High order multipoles)*
- Ament et al., Rev. Mod. Phys. **83**, 705 (2011) *(RIXS)*

INGREDIENTS FOR MAGNETISM

Intra atomic magnetic properties

- Isolated single ion
- Open shell (magnetic elements)
- Fine structure
  - ex. Rare Earth compounds

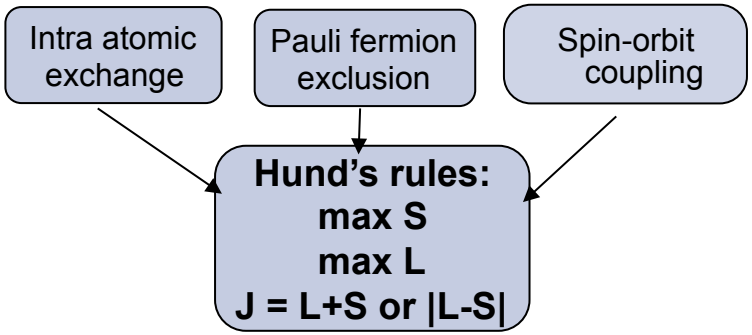

Crystal electric field perturbs the atomic magnetism

- Coulomb repulsion vs hopping transfer
- Breaking of Hund rules
- Quenching of orbital momentum
- Magnetic anisotropy
  - ex. Transition metal oxides

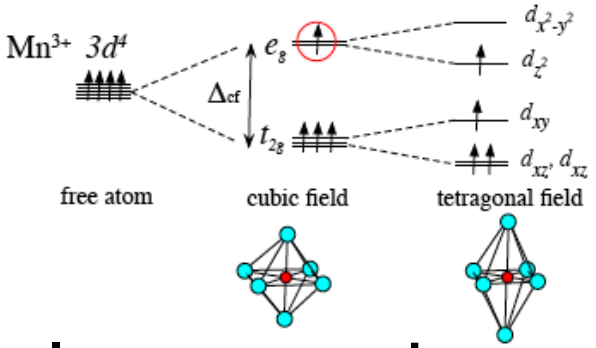

Inter atomic magnetic interactions induce long range order

- Isotropic exchange H=J **S**·**S** (Heisenberg)
- Anisotropic exchange H=**S** J **S** (Dzyaloshinsky-Moriya)
- Super-exchange and double-exchange
- Itinerant exchange (RKKY)

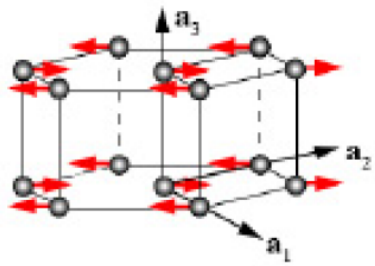

ELASTIC DIFFRACTION IN CRYSTALS

Interference between the resultatant waves diffused from each atom in the unit cell for any given reciprocal lattice vector **Q=G**$_{hkl}$

Differential cross section:

$$\left(\frac{d\sigma}{d\Omega}\right)_{Bragg} = N\frac{(2\pi)^3}{v_0}\sum_{hkl}\delta(\mathbf{Q}-\mathbf{G}_{hkl})\;|F(hkl)|^2$$

N° unit cell *unit cell volume* ***Laue's condition***

$$F(hkl) = \sum_s f_s\; e^{i\mathbf{G}_{hkl}\cdot\mathbf{d}_s - W_s}$$

Structure factor*: information about the atom distribution inside the unit cell*

$$f_s = \int_{atom}\rho_s(\mathbf{r}')e^{-i\mathbf{Q}\cdot\mathbf{r}'}d\mathbf{r}'$$

atomic scattering amplitude *for the atoms s related to the Fourier transform of the atomic electron density*

DESCRIPTION OF A MAGNETIC STRUCTURE

The magnetic propagation vector $\mathbf{q}_m$ describes the periodicity of a magnetic structures

Definition:

- q_m *is a reciprocal lattice vector*
- q_m *is a eigenfunction of the Translational Group*
- *It is defined inside the 1st Brillouin zone*
- *Perpendicular to the planes containing atoms with the same orientation of the magnetic moments*
- *The inverse of its modulus is equal to magnetic periodicity (Ex. $2\pi/q_m=2a$)*

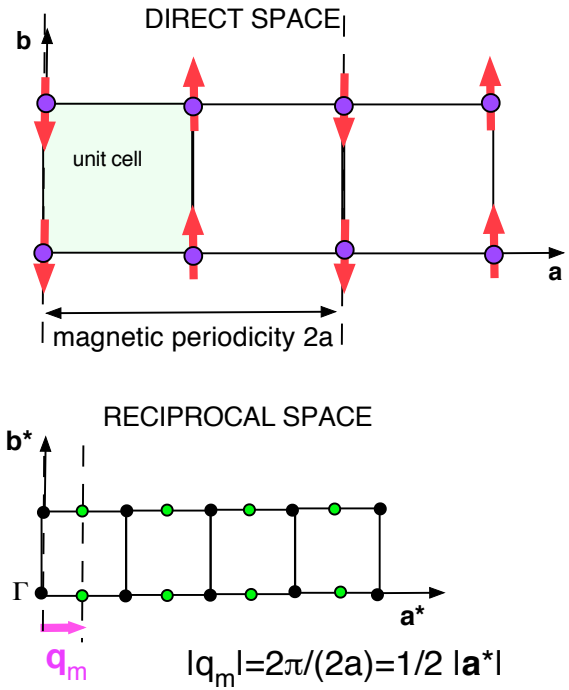

The **magnetic propagation** vector gives no information on the orientation of the magnetic moments

MAGNETIC MOMENT DISTRIBUTION

The magnetic moment distribution $\mathbf{m_{ns}}$ gives information about the magnetic moment direction of the s-atom inside the nth-lattice cell

$$\mathbf{m}_{ns} = \sum_{\mathbf{q}_m} \mathbf{m}_s^{\mathbf{q}_m} \; e^{-i\mathbf{q}_m \cdot \mathbf{R}_n}$$

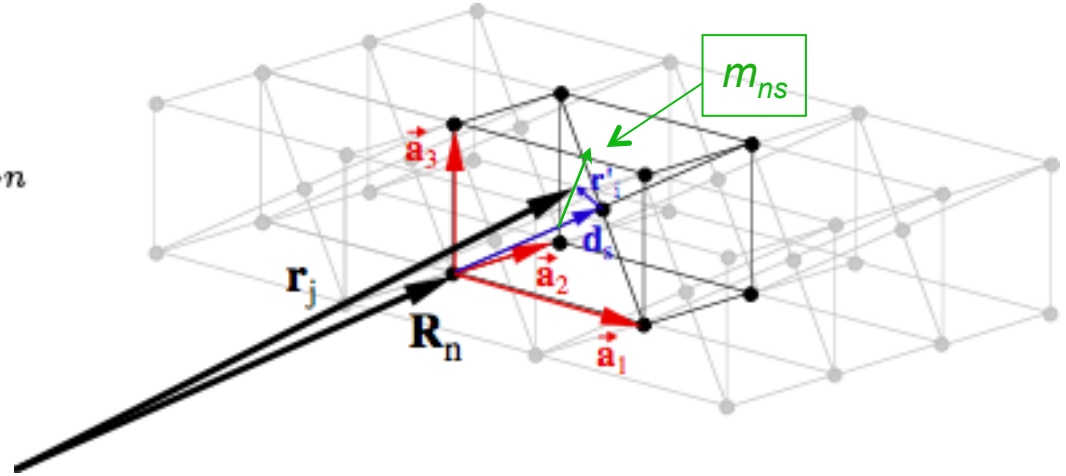

m_{ns} is a REAL vector defined in the direct space

- The fase factor is real ONLY if q_m correspond to the 1st Brillouin surface (i.e. for ferro and antiferromagnetics)

- In general the for any q_m the sum must include $-q_m$ such that :

$$\mathbf{m}_{ns} = \mathbf{m}_s^{\mathbf{q}_m} \; e^{-i\mathbf{q}_m \cdot \mathbf{R}_n} + \mathbf{m}_s^{-\mathbf{q}_m} \; e^{i\mathbf{q}_m \cdot \mathbf{R}_n} = 2 \left|\mathbf{m}_s^{\mathbf{q}_m}\right| \; \hat{\mathbf{u}} \; cos(\mathbf{q}_m \cdot \mathbf{R}_n + \phi)$$

EX : FERROMAGNETIC q_m=(000)

- All the magnetic moment m_j are parallel each others
- The magnetic and the chemical unit cells coincide
- Structural and magnetic reflections coincide

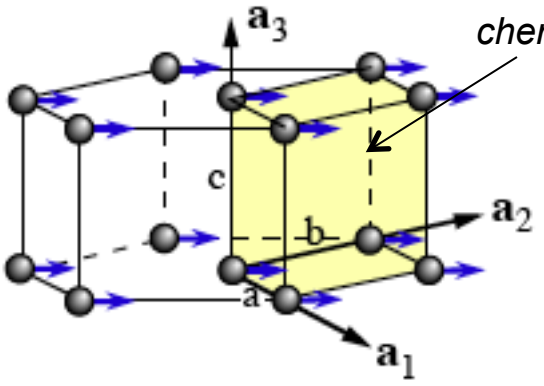

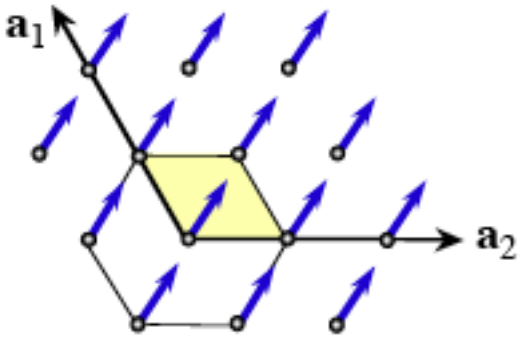

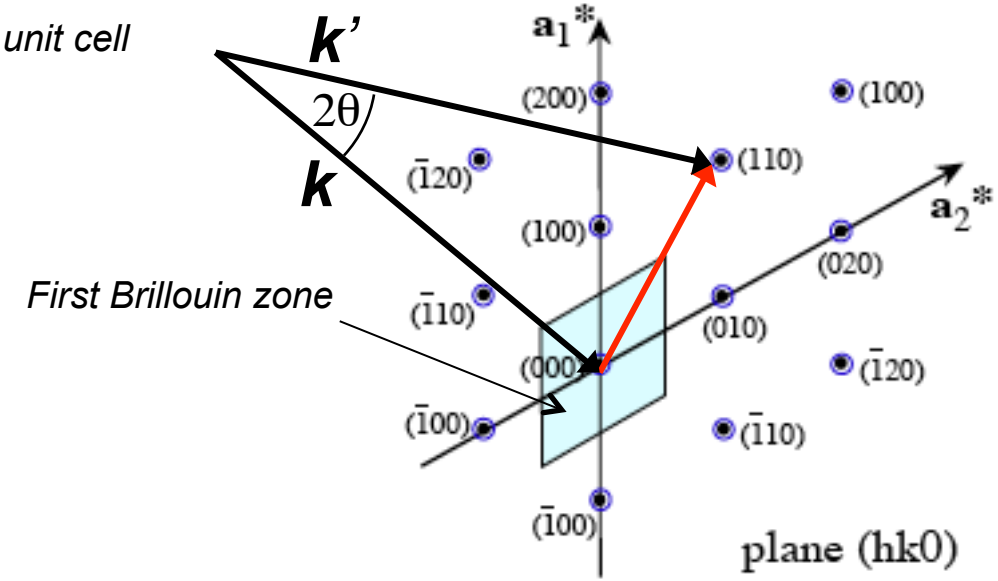

$\mathbf{q}_m$=(0,0,0)

$\mathbf{m}_{ns}$= $\mathbf{m}_0$ = $m_{01}\mathbf{a}_1$+m_{02} $\mathbf{a}_2$

EX : ANTIFERROMAGNETIC $q_m=(½ ,½ , 0)$

- Adjacent planes contain antiparallel magnetic moment $\mathbf{m}_j$
- Magnetic cell multiple of the chemical unit cell (double)
- Magnetic reflections correspond to the symmetry points at the surface of the Brillouin zone

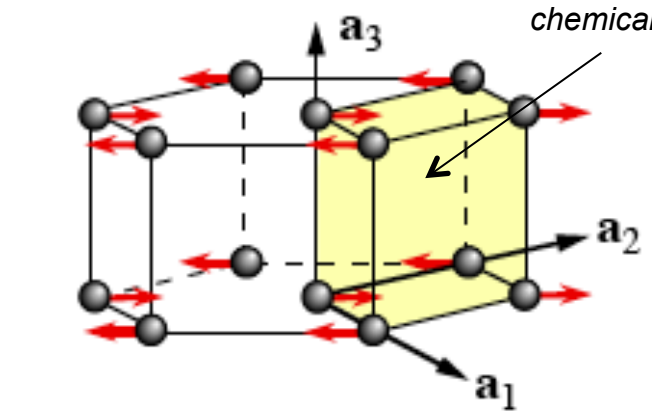

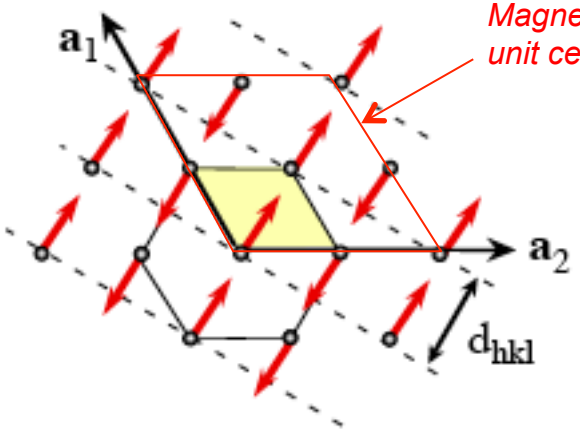

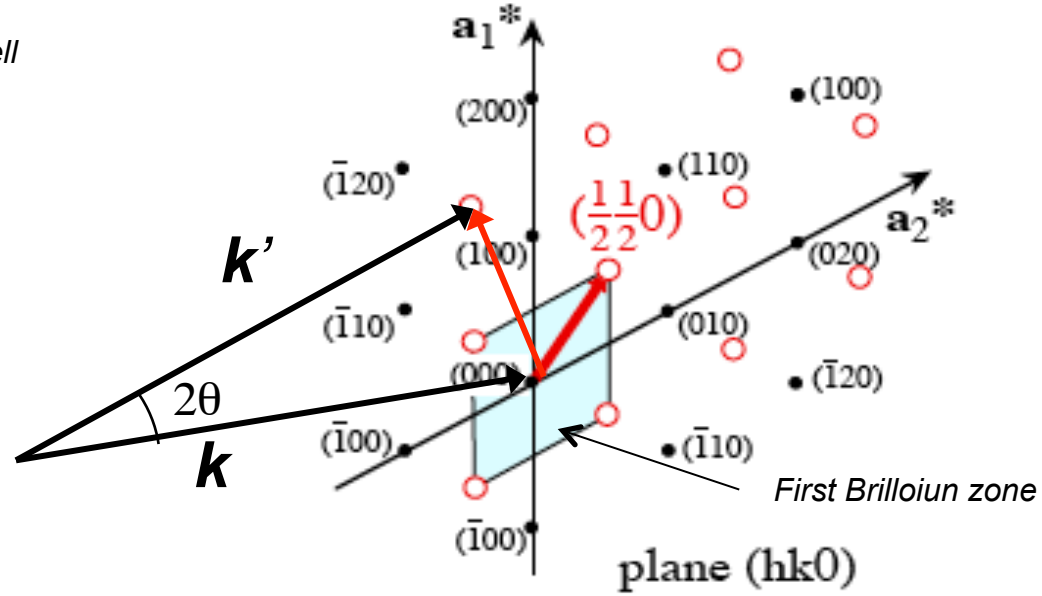

$\mathbf{q}_m=(½ , ½ ,0)$

$\mathbf{m}_{ns}=(-)^n \mathbf{m}_0 =(-)^n (m_{01}\mathbf{a}_1+m_{02}\mathbf{a}_2)$

EX : HELICAL $q_m=(0, 0, 1/3)$

- Propagation vector $\mathbf{q}_m$ have a non-integral periodicity
- In general both $\mathbf{q}_m$ and $-\mathbf{q}_m$ exists (indicated τ^+ and τ^-)

The propagation vector $\mathbf{q}_m$ inside the 1st Brillouin zone

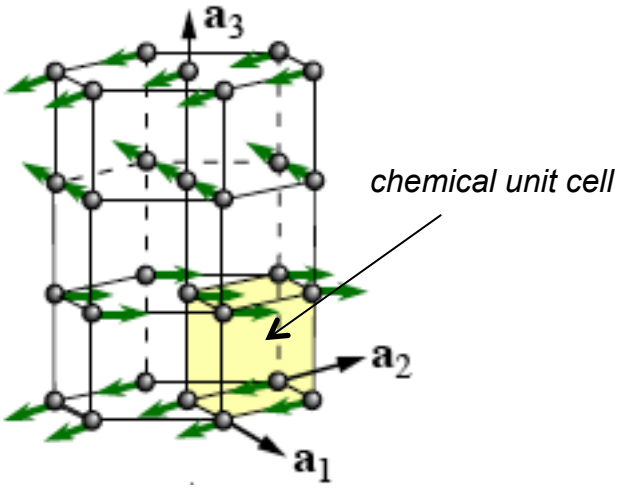

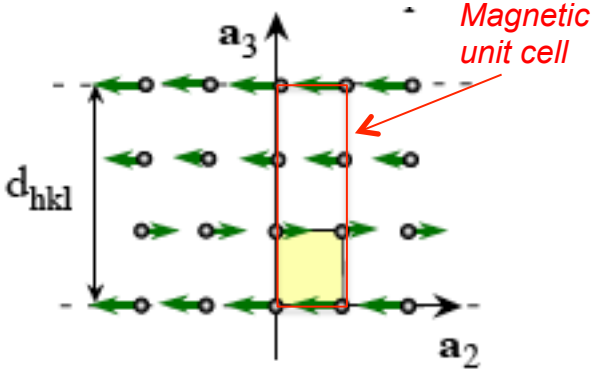

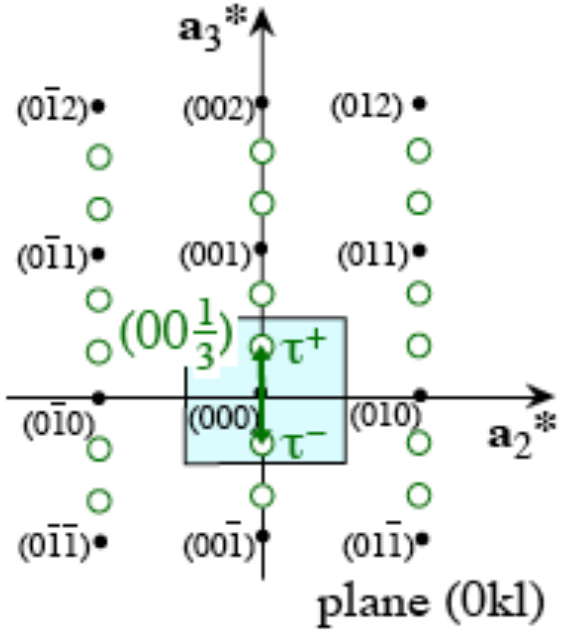

$\mathbf{q}_m=(0,0,1/3)$

$\mathbf{m}_{ns}=m_0[\cos(\mathbf{q}_m\cdot\mathbf{R}_n+\phi)\mathbf{u}_s+\sin(\mathbf{q}_m\cdot\mathbf{R}_n+\phi)\mathbf{v}_s]$

MODULATED STRUCTURES

Non-collinear incommensurate magnetic modulations

a) Simple helix

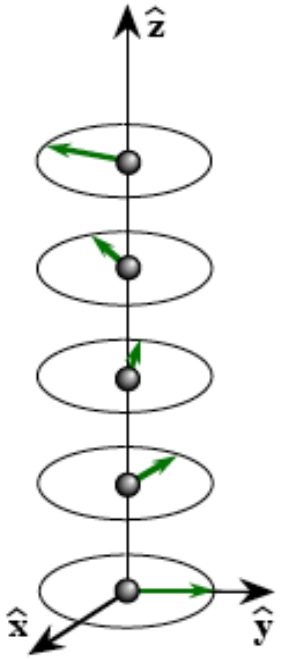

$$m_x = m_0 \cos\theta$$
$$m_y = m_0 \sin\theta$$
$$m_z = 0$$

b) Ferromagnetic helix

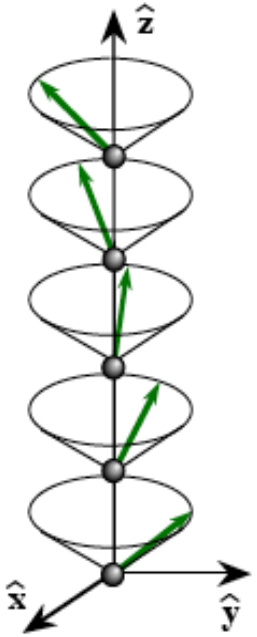

$$m_x = m_0 \cos\theta$$
$$m_y = m_0 \sin\theta$$
$$m_z \neq 0$$

c) Complex helix

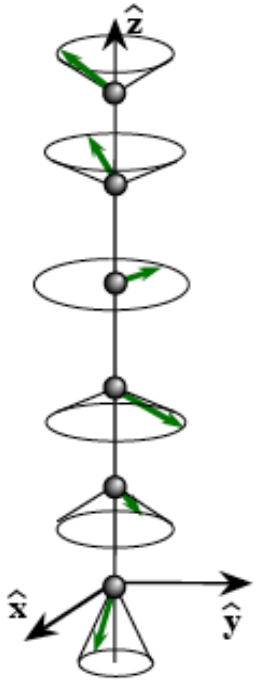

$$m_x = m_0 \cos\theta \sin\beta$$
$$m_y = m_0 \sin\theta \sin\beta$$
$$m_z = \cos\beta$$

ELECTRONIC GROUND STATE PROPERTIES

Charge density

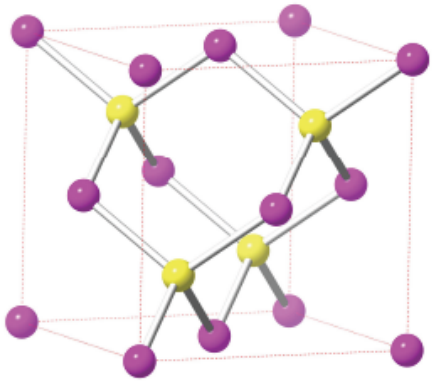

Charge order

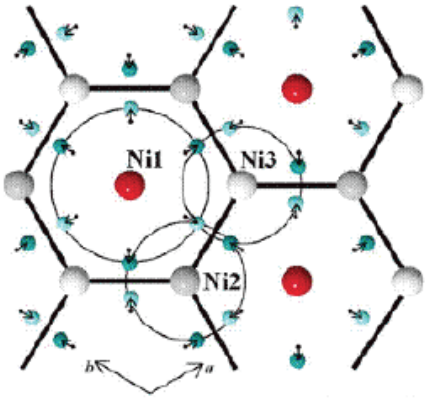

Magnetic order

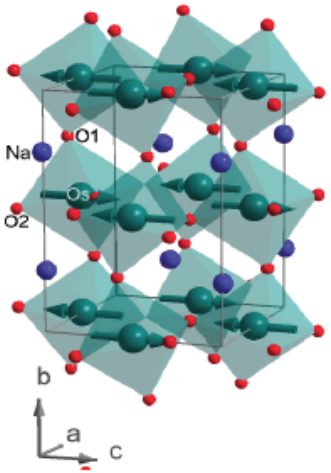

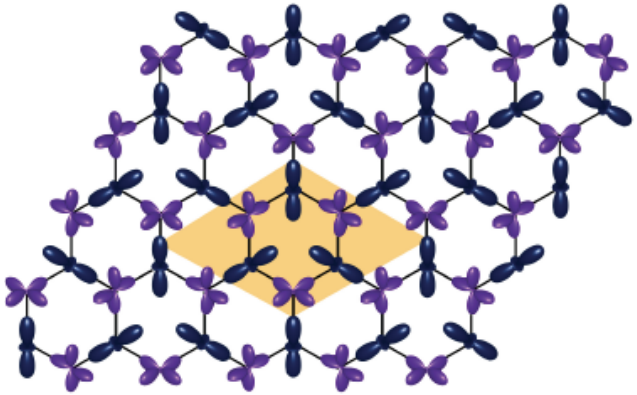

Orbital order

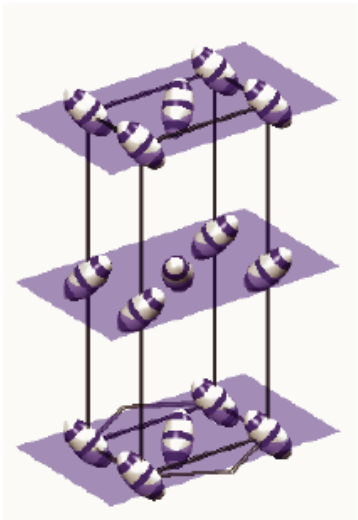

Quadrupolar order

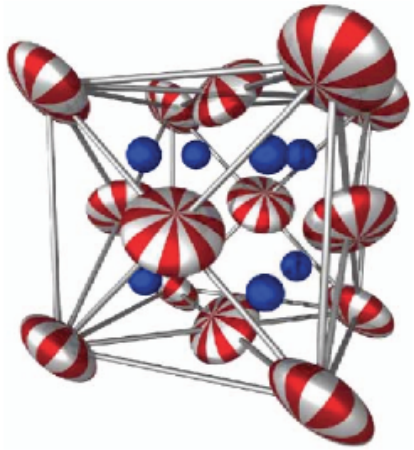

Octupolar order

X-RAYS PROPERTIES

Intrinsic properties

- Wave-Like and particle-like properties
- Rest mass: $m_{ph} = 0$
- Charge = 0
- Spin = 1
- Magnetic moment: $\mu_{ph} = 0$
- Polarization ε // Electric field **E**

Transverse EM waves

$$\vec{\mathbf{E}}(\vec{\mathbf{r}},t) = \hat{\epsilon}E_0 e^{i(\vec{\mathbf{k}}\cdot\vec{\mathbf{r}}-\omega t)}$$

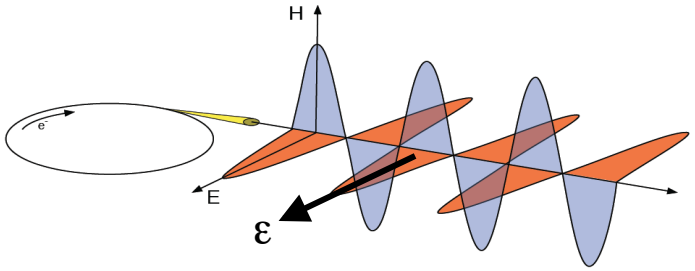

X-rays are electromagnetic waves and interact with the the electric **E** and the magnetic field **B** generated by the electrons

The electric **E** and magnetic **B** in term of scalar Φ and vector **A** potential

Maxwell equations

$$\mathbf{B} = \nabla \times \mathbf{A}$$

$$\mathbf{E} = -\nabla\Phi - \frac{1}{c}\frac{\partial \mathbf{A}}{\partial t}$$

Vector potential

$$\mathbf{A} = \mathbf{A}_0 e^{i(\mathbf{k}\cdot\mathbf{r}-\omega t)}$$

$$\mathbf{E} = \mathbf{E}_0 e^{i(\mathbf{k}\cdot\mathbf{r}-\omega t)}$$

$$\mathbf{B} = \mathbf{B}_0 e^{i(\mathbf{k}\cdot\mathbf{r}-\omega t)}$$

Energy

$\mathcal{E}$ [keV] = $\hbar\omega = hc/\lambda$ = 12.398 / λ [Å]

Spectral intensity

$I_0(\omega) = \langle E_0^2 \rangle = N(\omega)\,\hbar\omega$

ex. 1 Å = 12.398 keV

X-RAY-MATTER INTERACTIONS

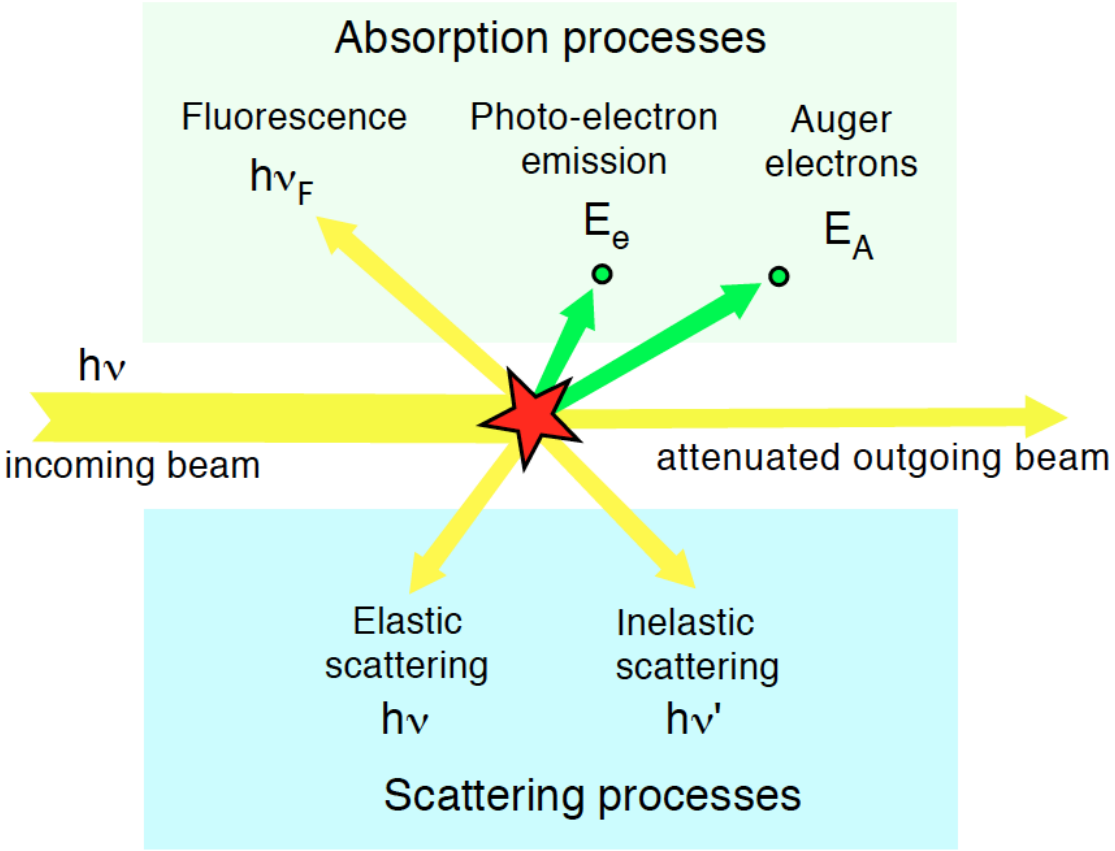

Photon absorption : Excitation with or without emission of electrons

Photon scattering :

Elastic	=> Thomson and magnetic
Inelastic	=> Compton (Raman)
Resonant	=> elastic or inelastic

X-RAYS CROSS SECTIONS

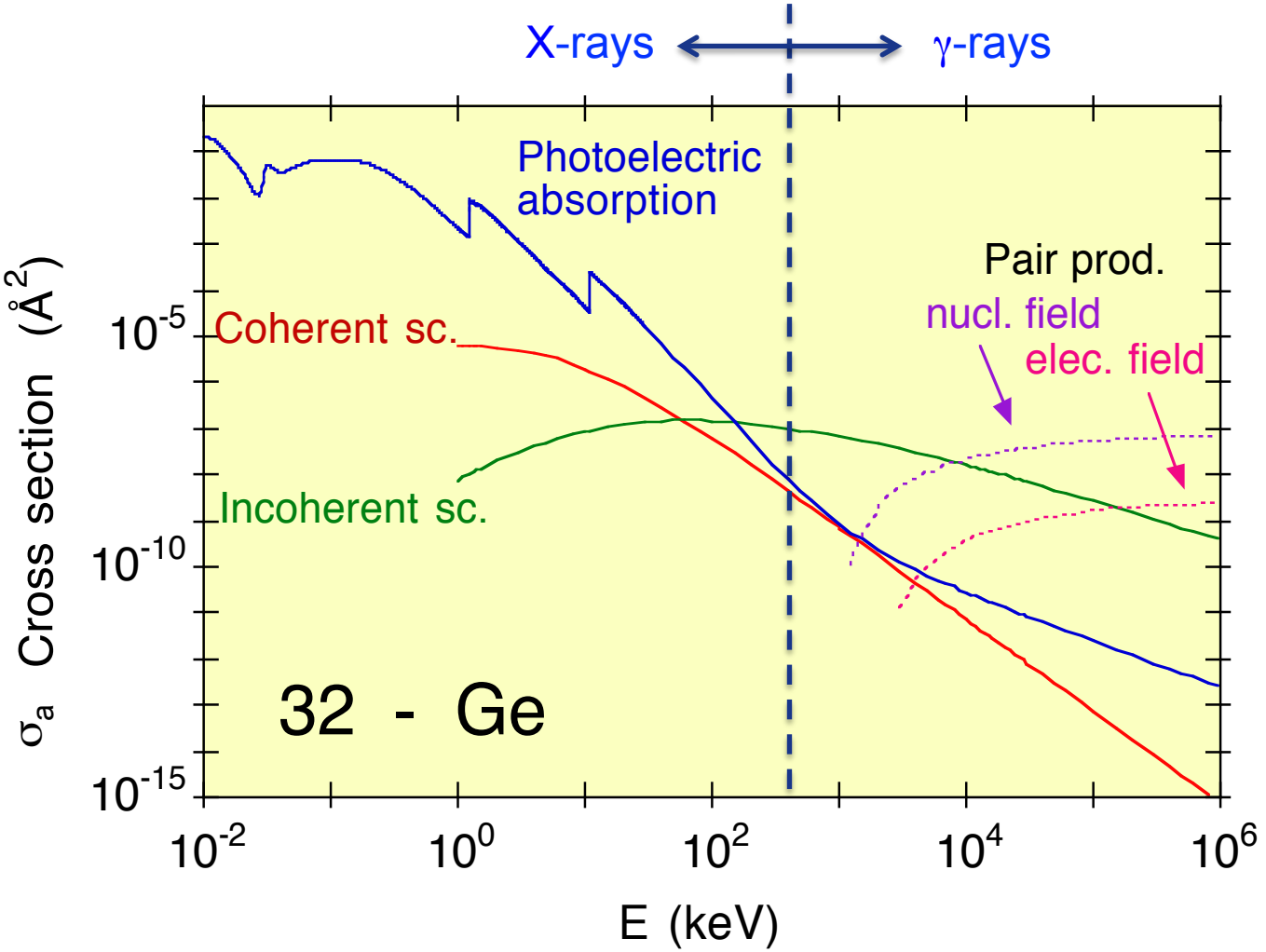

X-RAY SCATTERING BY FREE ELECTRONS

- The electron are at rest
- The electric field E_{in} of the incident x-rays act as a force **F**=**E**q
- The electron accelerates and radiates a spherical wave E_{rad}

Istantanous radiated spherical field E_{rad} :
- proportional to the electron acceleration
- anti-phase with respect E_{in}
- decreases with cos(ψ)

$$\frac{\mathrm{E_{rad}}(R,t)}{\mathrm{E_{in}}} = -\left(\frac{e^2}{4\pi\epsilon_0 mc^2}\right)\frac{\mathrm{e}^{ikR}}{R}\cos\psi$$

Thomson scattering length (Lorentz radius):

$$r_0 = \left(\frac{e^2}{4\pi\epsilon_0 mc^2}\right) = 2.82\times10^{-5}\ \text{Å}$$

m = electron mass
e = electron charge

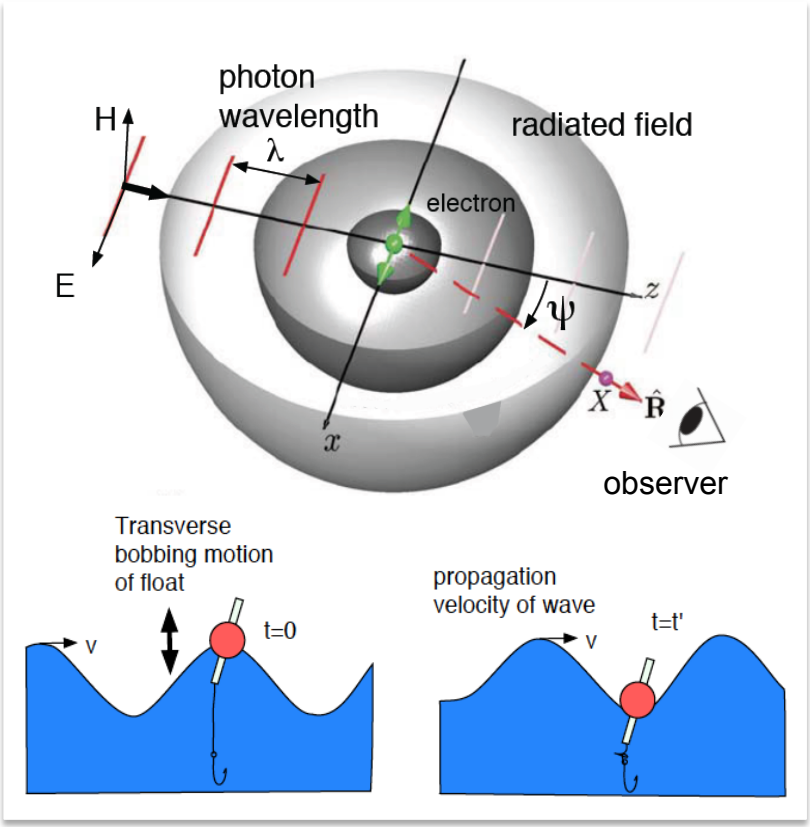

POLARIZATION DEPENDENCE OF X-RAYS

The differential cross section for the Thomson scattering depends from the incident and scattered photon polarizations

$$\left(\frac{d\sigma}{d\Omega}\right) = r_0^2 \left|\hat{\boldsymbol{\varepsilon}} \cdot \hat{\boldsymbol{\varepsilon}}'\right|^2 \qquad P = \left|\hat{\boldsymbol{\varepsilon}} \cdot \hat{\boldsymbol{\varepsilon}}'\right|^2 = \begin{cases} 1 & \text{synchrotron: vertical scattering plane} \\ \cos^2\psi & \text{synchrotron: horizontal scattering plane} \\ \frac{1}{2}\left(1+\cos^2\psi\right) & \text{unpolarized source} \end{cases}$$

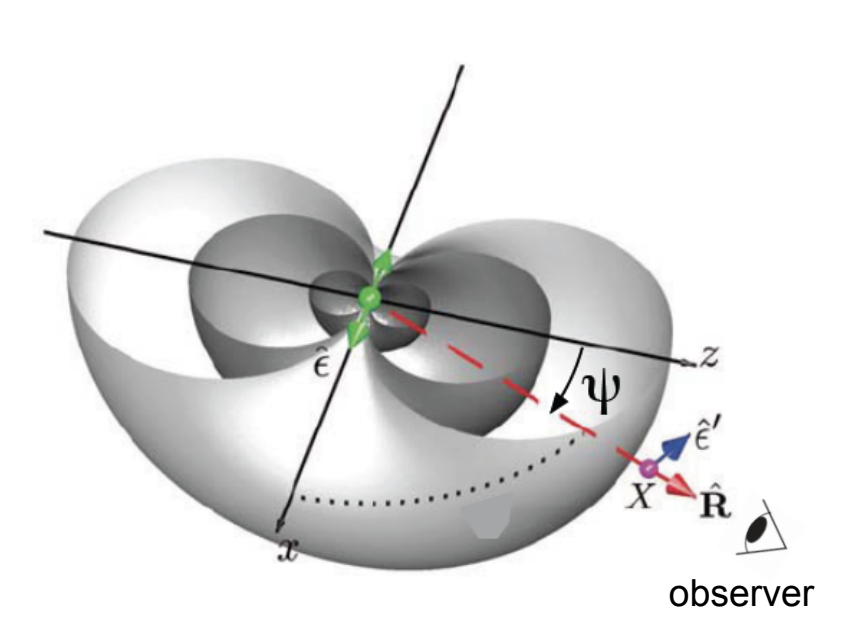

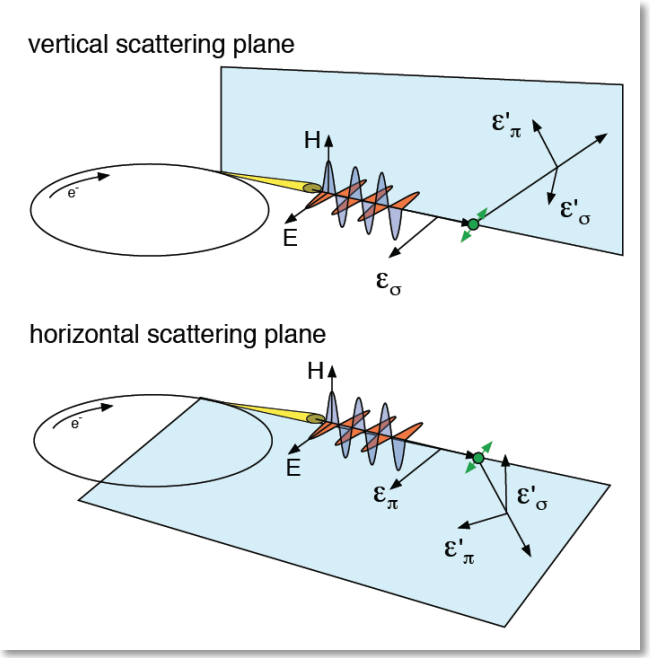

X-RAY MAGNETIC SCATTERING

The magnetic interaction is a relativistic correction to the Thomson scattering

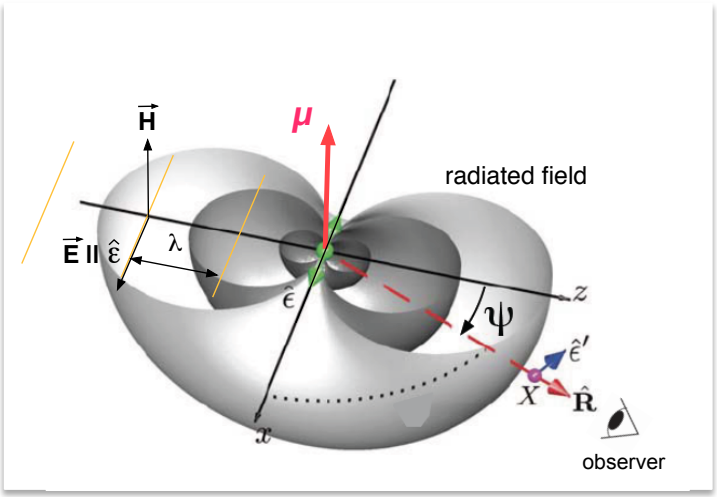

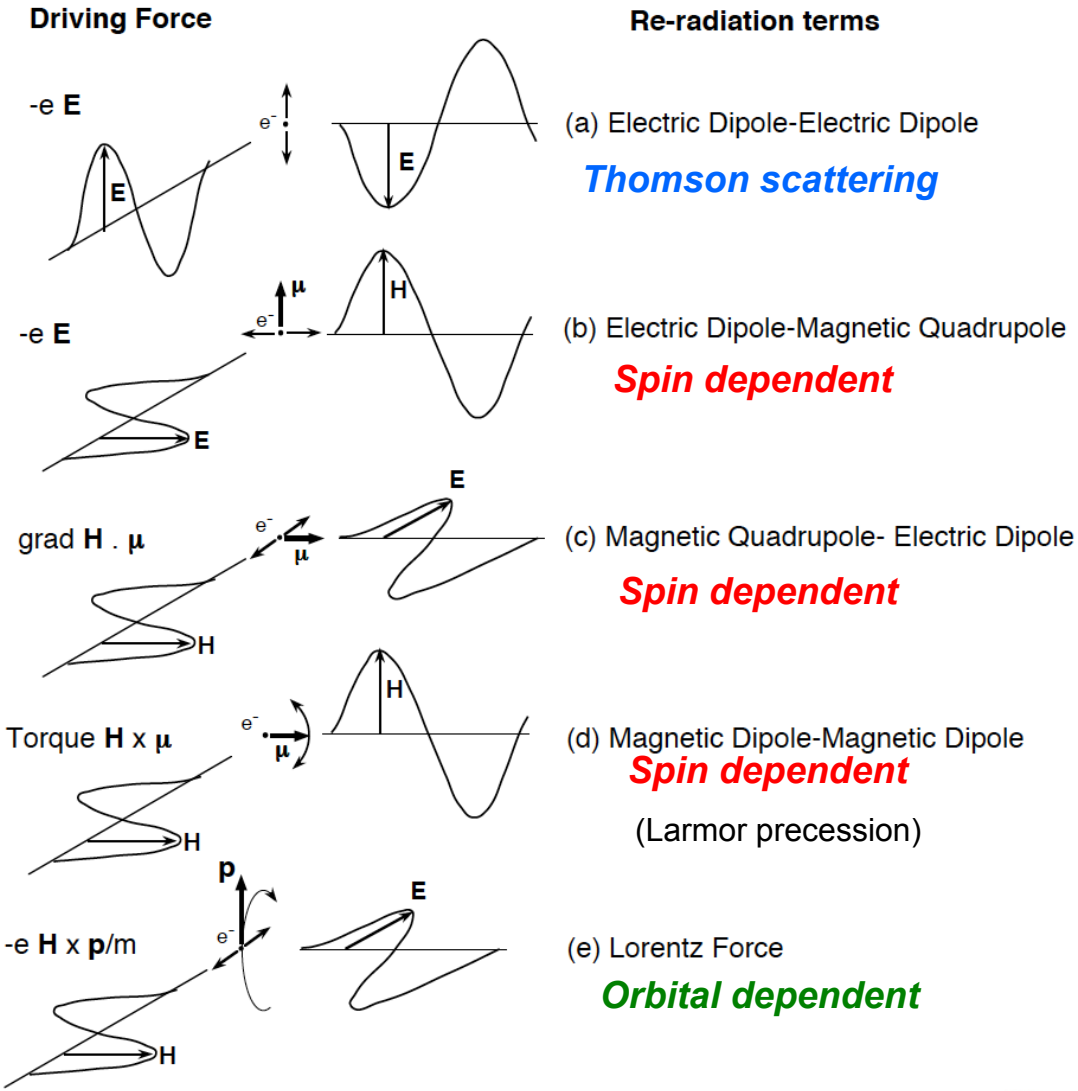

de Bergevin and Brunel (Acta Cryst., 1981)

HISTORY OF X-RAY MAGNETIC SCATTERING

Theory photon-electron interaction

- Klein & Nishina: Compton scattering (1929)
- Bohr (1932)
- Gell-Mann & Goldberg (1954)
- Lowe (1955)

Pre-synchrotron works

- Platzman & Tzoar: Theory (1972)
- de Bergevin & Brunel: Theory and Exp.NiO, Fe_2O_3, MnO (1972,1981,1984)

2nd generation synchrotron works

Resonant Exchange scattering

- Blume (1985)
- Gibbs, Bohr, Moncton: Exp. Ho (1985,1986)
- Namikawa: Exp. Ni (1985)
- Hannon, Trammel, Blume, Gibbs: theory (1988)
- Vettier, Isaac, McWhan: Exp. UAs (1989)

Magnetic circular dichroism

- Shutz: Exp. XMCD Fe (1987)
- Carra & Altarelli: Theory (1989)

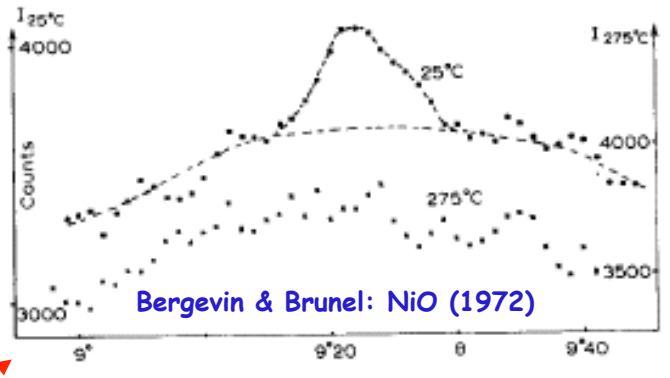

D. Gibbs et al.: Ho L-edge (1985)

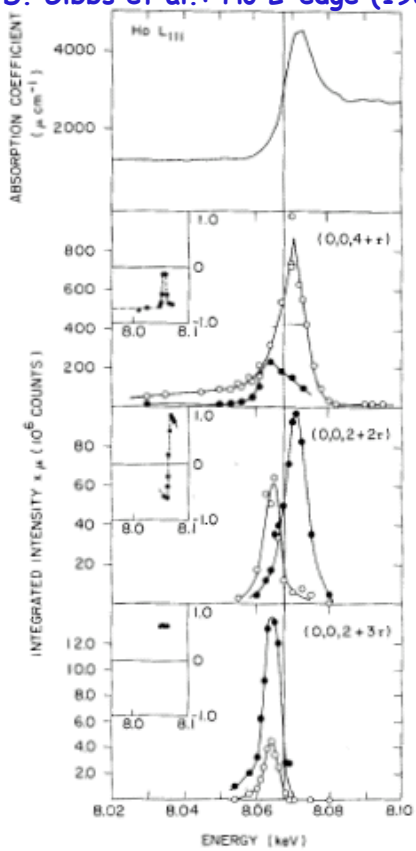

G. Shutz: Fe K-edge (1987)

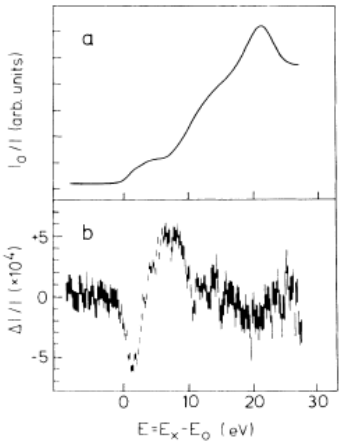

SCATTERING FROM BOUND ELECTRONS

The bound electron is subject to the electric field E_{in} of an incident X-ray beam and to a damping term proportional to the electron velocity $\Gamma\dot{x}$ which represents dissipation of energy.

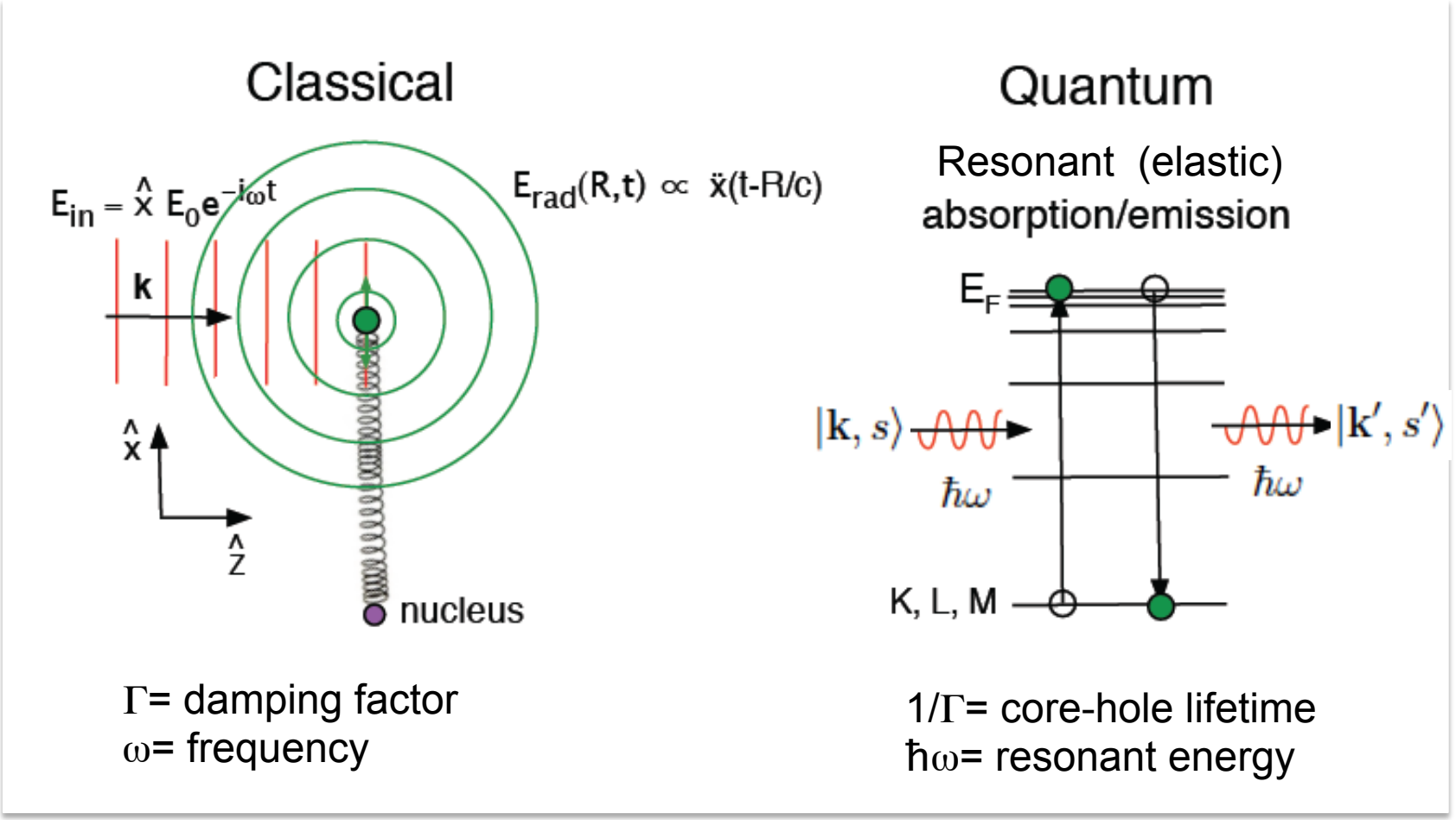

Γ= damping factor
ω= frequency

$1/\Gamma$= core-hole lifetime
$\hbar\omega$= resonant energy

DISPERSION CORRECTIONS

Because the electrons are bound in atoms with discrete energies, a more elaborate model than that of a cloud of free electrons must be invoked.

The scattering amplitude includes two energy dependent term f'(ω) and f"(ω) which are called "dispersion corrections".

$$f(\mathbf{Q},\omega) = f^0(\mathbf{Q}) + f'(\omega) + i\,f''(\omega)$$

The dispersion corrections are derived by treating atomic electrons as harmonic oscillators. The absorption cross section σ_a is a superposition of oscillators with relative weights, so-called oscillator strengths, $g(\omega_s)$, proportional to $\sigma_a(\omega = \omega_s)$.

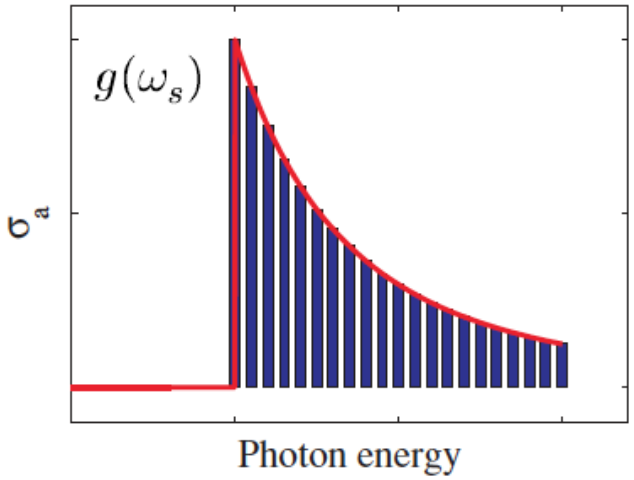

QUANTUM DESCRIPTION OF MATTER

Matter is described by a wavefunction Ψ solution of **Schrodinger equation**:

$$H\,\Psi = E\,\Psi \qquad \Psi(r_1, r_2, \ldots r_n; R_1, R_2, \ldots R_N)$$

r_i electron positions R_i Nuclei positions

1) **Born-Oppenheimer approximation:**
   Nuclei at the rest position R_i^0
   An effective Hamiltonian H_{eff} describes the attractive potential of ions on the electrons
2) **Mean field approximation:**
   Electrons move independently in the mean field created by the other electrons
   No electron correlation effects and Ψ depends only from $\mathbf{r}_j$
3) **One electron approximation:**
   The wavefunction of the electron $\mathbf{r}_n$ can be single out
   The effective Hamiltonian depends only from the coordinate of this electron

$$\Psi(r_1, r_2, \ldots r_n; R_1^0, R_2^0, \ldots R_N^0) \sim \Psi(r_1, r_2, \ldots r_{n-1}; R_1^0, R_2^0, \ldots R_N^0)\,\psi(r_n)$$

$$H_{eff}(\mathbf{r}_n)\,\psi(r_n) = E\,\psi(r_n)$$

QUANTUM DESCRIPTION OF X-RAYS

Quantization of the electromagnetic field

The “second quantization” describes the EM field as photon states with an occupation number “n”, wavevector **k** and polarization “ε”,

$$|n_{k_1,\epsilon_1}; ...n_{k,\epsilon}; ...n_{k_t,\epsilon_t}\rangle$$

and the **creation** and **annihilation** operators, “$a^\dagger$” and “a” defined as:

$$a^\dagger_{k,\epsilon}|n_{k_1,\epsilon_1}; ...n_{k,\epsilon}; ...n_{k_t,\epsilon_t}\rangle = \sqrt{n_{k,\epsilon}+1}|n_{k_1,\epsilon_1}; ...n_{k,\epsilon}+1; ...n_{k_t,\epsilon_t}\rangle$$

$$a_{k,\epsilon}|n_{k_1,\epsilon_1}; ...n_{k,\epsilon}; ...n_{k_t,\epsilon_t}\rangle = \sqrt{n_{k,\epsilon}}|n_{k_1,\epsilon_1}; ...n_{k,\epsilon}-1; ...n_{k_t,\epsilon_t}\rangle$$

With this assumptions, the harmonic components of an EM field is decomposed in a sum of quantized oscillators. The vector potential **A** then became an operator:

$$\mathbf{A}(\mathbf{r},t) = \sum_{k,\epsilon}\sqrt{\frac{4\pi\hbar c^2}{2V\omega_k}}\left(a_{k,\epsilon}\hat{\epsilon}_{k,\epsilon}e^{i\mathbf{k}\cdot\mathbf{r}-i\omega t} + a^\dagger_{k,\epsilon}\hat{\epsilon}^*_{k,\epsilon}e^{-i\mathbf{k}\cdot\mathbf{r}-i\omega t}\right)$$

THEORY X-RAYS MATTER INTERACTION

1) **Interaction occurs mainly with the electrons**
   we considers only the electronic transitions
   we suppose to know their eigenstates and the eigenfunctions
2) **The system is composed by N identical microscopic entities**
   Atoms, molecules, clusters …
3) **The electromagnetic wave acts as a time-dependent perturbation**
   modify the electron wavefunction
   transitions between eigenstates

FERMI GOLDEN RULE (second order)

Transition rate W_{fi} per unit of volume between an initial $|\Psi_i\rangle$ and a final $\langle\Psi_f|$ unperturbed eigenstate

$$W_{fi} = \frac{2\pi}{\hbar}\left|\langle\Psi_f|H_{int}|\Psi_i\rangle + \sum_k \frac{\langle\Psi_f|H_{int}|\Psi_k\rangle\langle\Psi_k|H_{int}|\Psi_i\rangle}{E_i - E_k - \hbar\omega}\right|^2 \delta(E_f - E_i - \hbar\omega)$$

The interaction Hamiltonian H_{int} describes the relativistic behaviour of electrons in an electromagnetic field

RELATIVISTIC INTERACTIONS

The interaction Hamiltonian is obtained from the **Dirac equation** in the limit of low velocities and taking the terms $o(v/c)$.

Relativistic terms

$$\hat{H}_{int} = \sum_j \left(-\frac{e}{mc}\mathbf{A}(\mathbf{r}_j)\cdot\mathbf{p}_j + \frac{e^2}{2mc^2}\mathbf{A}^2(\mathbf{r}_j) - \frac{e\hbar}{mc}\mathbf{s}_j\cdot\nabla\times\mathbf{A} - \frac{e\hbar}{2m^2c^3}\mathbf{s}_j\cdot\frac{\partial\mathbf{A}}{\partial t}\times\frac{e}{c}\mathbf{A} \right)$$

Zeeman term:
Interaction of electron spins s_j with the magnetic field **H**

Spin orbit interaction:
interaction between the spin **S** and the orbital part **L** of the electron's wave functions

$$H_{so} = -\frac{1}{2}\,\mu\cdot\mathbf{B}^p = \frac{e\hbar^2}{2m_e c^2 r}\frac{dV(r)}{dr}\,\mathbf{L}\cdot\mathbf{S} = \lambda\,\mathbf{L}\cdot\mathbf{S}$$

RELATIVISTIC SCATTERING THEORY

For a complete description of the x-ray-matter interaction we need to consider the **relativistic motion of the electrons in a quantized electromagnetic field.**

- Non-interacting electrons H_{el}

$$\mathcal{H}_{el} = \sum_j \frac{1}{2m}\mathbf{P}_j^2 + \sum_{ij} V(r_{ij}) + \frac{e\hbar}{2(mc)^2}\sum_j \mathbf{s}_j \cdot (\nabla\Phi_j \times \mathbf{P}_j),$$

- Non-interacting photons H_{ph}

$$H_{phot} = \sum_{\mathbf{k},\epsilon} \hbar\omega(a^\dagger_{k,\epsilon}a_{k,\epsilon} + \frac{1}{2})$$

Spatial part of vector potential

$$\mathbf{A}(\mathbf{r}_j) = \hat{\epsilon}\sqrt{\frac{\hbar}{2\epsilon_0 V\omega}}\left[a_{k,s}e^{i\mathbf{k}\cdot\mathbf{r}_j} + a^\dagger_{k,s}e^{-i\mathbf{k}\cdot\mathbf{r}_j}\right]$$

- Interaction term H'

$$\begin{aligned}\mathcal{H}' &= \mathcal{H}'_1 + \mathcal{H}'_2 + \mathcal{H}'_3 + \mathcal{H}'_4 \\ &= \frac{e^2}{2mc^2}\sum_j \mathbf{A}^2(\mathbf{r}_j) \\ &\quad -\frac{e}{mc}\sum_j \mathbf{A}(\mathbf{r}_j)\cdot\mathbf{P}_j \\ &\quad -\frac{e\hbar}{mc}\sum_j \mathbf{s}_j\cdot[\nabla\times\mathbf{A}(\mathbf{r}_j)] \\ &\quad -\frac{e\hbar}{2(mc)^2}\frac{e}{c^2}\sum_j \mathbf{s}_j\cdot[\dot{\mathbf{A}}(\mathbf{r}_j)\times\mathbf{A}(\mathbf{r}_j)].\end{aligned}$$

A^2: quadratic terms
(product of $a_{ks}^\dagger a_{k's'}$, $a_{ks}^\dagger a_{k's'}$, …)

A: linear terms
(single terms $a_{ks}^\dagger$ and a_{ks})

ELASTIC SCATTERING PROCESSES

Absorption processes => retain only the photon annihilation operator $a_{k,s}$ linear terms in the **A**

Scattering processes => involve both the photon operators $a_{ks}^{\dagger}$ and a_{ks} quadratic terms $\mathbf{A}^2$

Elastic scattering processes conserves the number of photons.

- 1st order perturbation: QUADRATIC terms in A(r) (H'_1 and H'_4)
- 2nd order perturbation: LINEAR terms in A(r) (H'_2 and H'_3)

Fermi's Golden rule:

$$W = \frac{2\pi}{\hbar} \left| < a\ ;\ \mathbf{k}'\ \epsilon' |\ H'_1 + H'_4\ | a\ ;\ \mathbf{k}\ \epsilon > + \sum_n \frac{< a\ ;\ \mathbf{k}'\ \epsilon' |\ H'_2 + H'_3\ | n >< n |\ H'_2 + H'_3\ | a\ ;\ \mathbf{k}\ \epsilon >}{E_a + \hbar\omega_k - E_n} \right|^2$$

1st order *2nd order*

$$|i\rangle = |a; \mathbf{k}, \epsilon\rangle, \quad |f\rangle = |b; \mathbf{k}', \epsilon'\rangle$$

X-RAYS SCATTERING AMPLITUDES

M. Blume, J. Appl. Phys. 57, 3615 (1985)
M. Blume,*"Resonant anomalous x-ray scattering"*, ed. G. Materlik, (1994).

$$f_0(\mathbf{Q},\hat{\epsilon},\hat{\epsilon}') = \langle a \mid \sum_j e^{i\mathbf{Q}\cdot\mathbf{r}_j} \mid a\rangle \hat{\epsilon}'\cdot\hat{\epsilon}.$$

Thomson
Charge density

$$f^{magn.}(\mathbf{Q}) = -i\frac{\hbar\omega_k}{mc^2}\left(\mathbf{L}(\mathbf{Q})\cdot\mathbf{P}_L + \mathbf{S}(\mathbf{Q})\cdot\mathbf{P}_S\right)$$

Non-resonant magnetic
Orbital and spin separation
Magnetization density

Polarization dependent terms

$$\mathbf{P}_L = -\sin^2\theta\,[\mathbf{Q}\times[(\hat{\epsilon}'^*\times\hat{\epsilon})\times\mathbf{Q}]]$$
$$\mathbf{P}_S = \hat{\epsilon}'^*\times\hat{\epsilon} + (\hat{\mathbf{k}}'\times\hat{\epsilon}'^*)(\hat{\mathbf{k}}'\cdot\hat{\epsilon}) - (\hat{\mathbf{k}}\times\hat{\epsilon})(\hat{\mathbf{k}}\cdot\hat{\epsilon}'^*) - (\hat{\mathbf{k}}'\times\hat{\epsilon}'^*)\times(\hat{\mathbf{k}}\times\hat{\epsilon})$$

$$f^{RXS} = +\frac{1}{m}\sum_c \frac{E_g - E_c}{\hbar\omega_k}\left(\frac{\hat{\epsilon}'^*\cdot\langle g|\,\tilde{O}^\dagger(\mathbf{k}')\,|c\rangle\,\langle c|\,\tilde{O}(\mathbf{k})\,|g\rangle\cdot\hat{\epsilon}}{E_g - E_c + \hbar\omega_k - i\Gamma_c/2} - \frac{\hat{\epsilon}\cdot\langle g|\,\tilde{O}(\mathbf{k})\,|c\rangle\,\langle c|\,\tilde{O}^\dagger(\mathbf{k}')\,|g\rangle\cdot\hat{\epsilon}'^*}{E_g - E_c - \hbar\omega_k}\right)$$

Resonant terms
Core-hole virtual transition
Tensorial amplitudes
High order multipoles

Current operators J(k)

$$\hat{O}(\mathbf{k}) = \sum_j e^{i\mathbf{k}\cdot\mathbf{r}_j}\,[\,\hat{\epsilon}\cdot\mathbf{P}_j - i\hbar(\mathbf{k}\times\hat{\epsilon})\cdot\mathbf{s}_j\,]$$
$$\hat{O}^+(\mathbf{k}') = \sum_j e^{-i\mathbf{k}'\cdot\mathbf{r}_j}\,[\,\hat{\epsilon}'\cdot\mathbf{P}_j + i\hbar(\mathbf{k}'\times\hat{\epsilon}')\cdot\mathbf{s}_j\,]$$

X-RAYS ELASTIC SCATTERING CROSS SECTIONS

Coherent elastic scattering cross-section for periodic crystals

$$\frac{d\sigma}{d\Omega} = r_0^2 \left| \sum_n e^{i\mathbf{Q}\cdot\mathbf{R}_n} f_n(\mathbf{k}, \mathbf{k}', \hat{\epsilon}, \hat{\epsilon}', \hbar\omega_k) \right|^2$$

n= unit cell atomic site

Site selectivity

- *Space group symmetries*
- *Extinction rules*

Atomic scattering amplitudes

- *Atomic properties (photon-electron interactions)*
- *Electronic order parameters*

$$f = f_0 + f^{magn.} + f' + if''$$

CHARGE (Thomson)
E=10-50 keV
Z r_0 ~ 1-95 r_0

Structural characterization

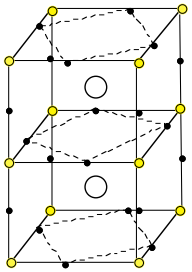

MAGNETIC
E=3.0-10 keV
$h\omega/mc^2$ $Z^{magn.}$ r_0 ~ 0.001-0.03 r_0

Magnetic structure determination

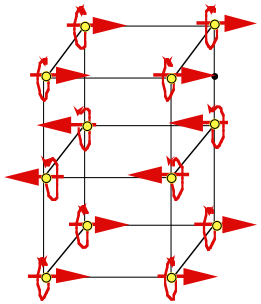

RESONANT
E=3-20 keV
$Z^{res.}$ r_0 ~ 0.01-100 r_0

Valence electron anysotropies

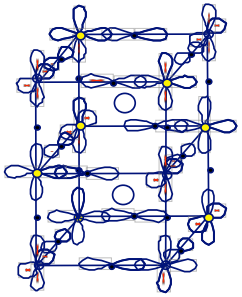

X-RAYS SCATTERING INTENSITIES

High-Q quality samples are required to detect the weak magnetic reflections

$$\frac{\sigma_{mag}}{\sigma_{charge}} \simeq \left(\frac{\hbar\omega_k}{mc^2}\right)^2 \left(\frac{N_m}{N}\right)^2 \langle M \rangle^2 \left(\frac{f_m}{f}\right)^2$$

~ 10^{-6} @ 9 keV

RESONANT

$I_{res.}$~10^3-10^5 cts/s

CHARGE (Thomson)

$I_{ch.}$~10^5-10^9 cts/s

MAGNETIC

$I_{magn.}$~10^0-10^2 cts/s

NON RESONANT X-RAYS MAGNETIC SCATTERING

The high-Q resolution allow the separation of crystallographic and magnetic reflections.

Ex. Charge and antiferromagnetic Bragg reflections in $Ce_{0.93}Co_{0.07}Fe_2$

Thomson scattering

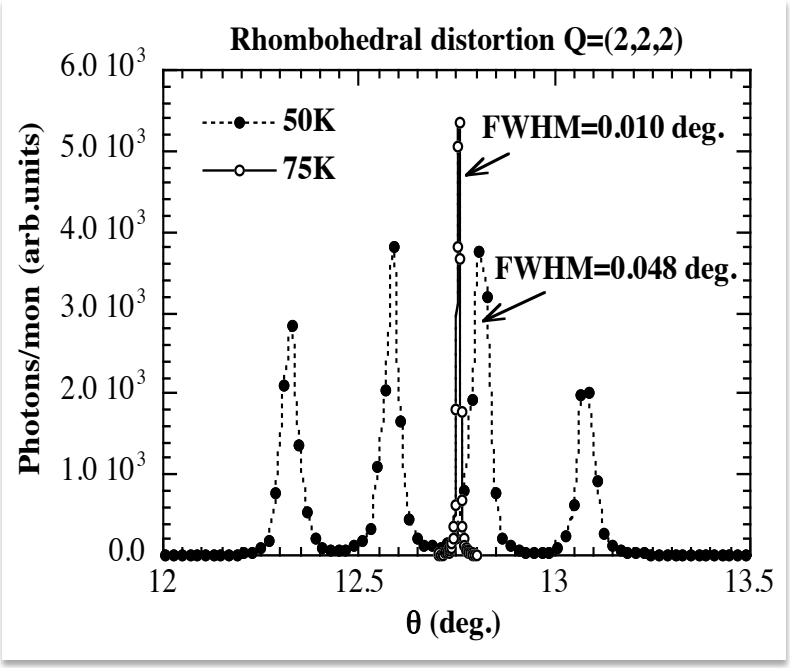

Non-resonant magnetic scattering

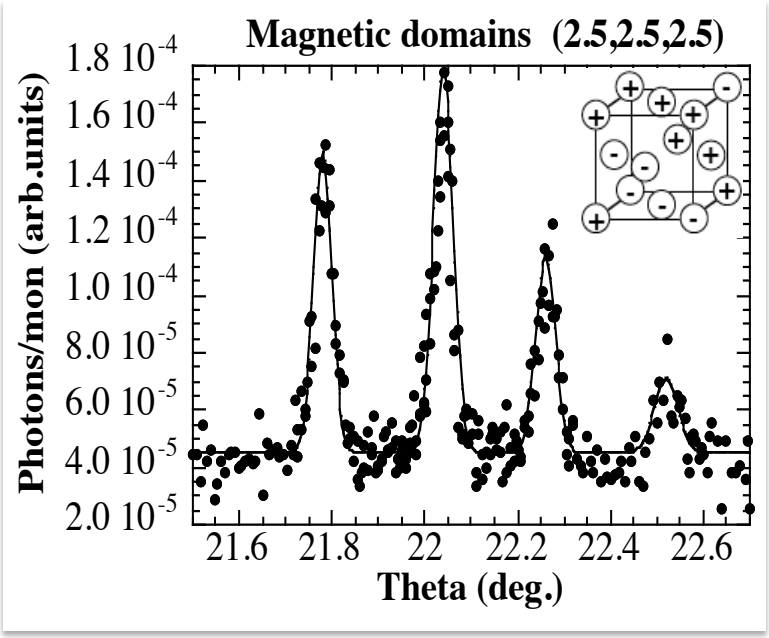

POLARIZED X-RAYS

X-rays Polarization analyser

- Thomson selection rules ($\varepsilon \cdot \varepsilon'$)
- Bragg diffraction by a crystal analyzer $2\theta_p$~90°
- η = rotation about scattered wavevector k'

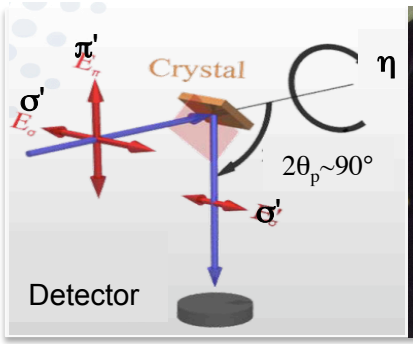

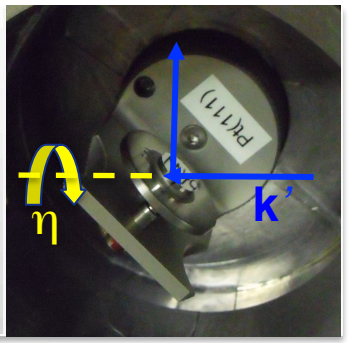

Phase plate retarder

Phase shift $\Delta\alpha$ between the transmitted and incident beam in the dynamical diffraction limit

$$\Delta\alpha = \frac{2\pi}{\lambda}(n_\sigma - n_\pi)d = -\frac{\pi}{2}\left[\frac{r_e^2\lambda^3 Re(F_h F_{\bar{h}})sin2\theta_{pp}}{\pi^2 V^2 \Delta\theta_{pp}}\right]d$$

Half wave plate mode ($\Delta\alpha=\pi$)
- Rotation of 90° of liner polarization (when χ=45°)

Quarter wave plate mode ($\Delta\alpha=\pi/2$)
-Circular left/right polarizations (~98-99%)

Linear Polarization Scan ($\Delta\alpha=\pi$)
-Continous rotation of χ

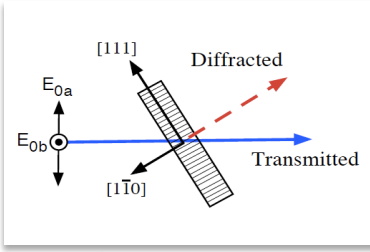

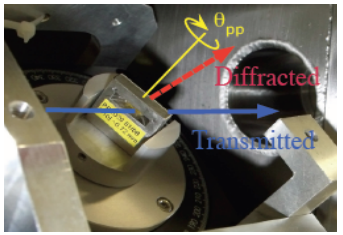

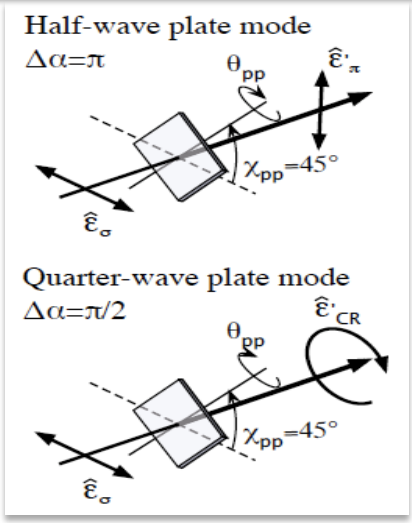

TYPICAL BEAMLINE FOR REXS (EX ID20-ESRF)

Paolasini, et al. J. Synchrotron Rad. 14 (2007) 301-312.

Azimuthal diffractometer

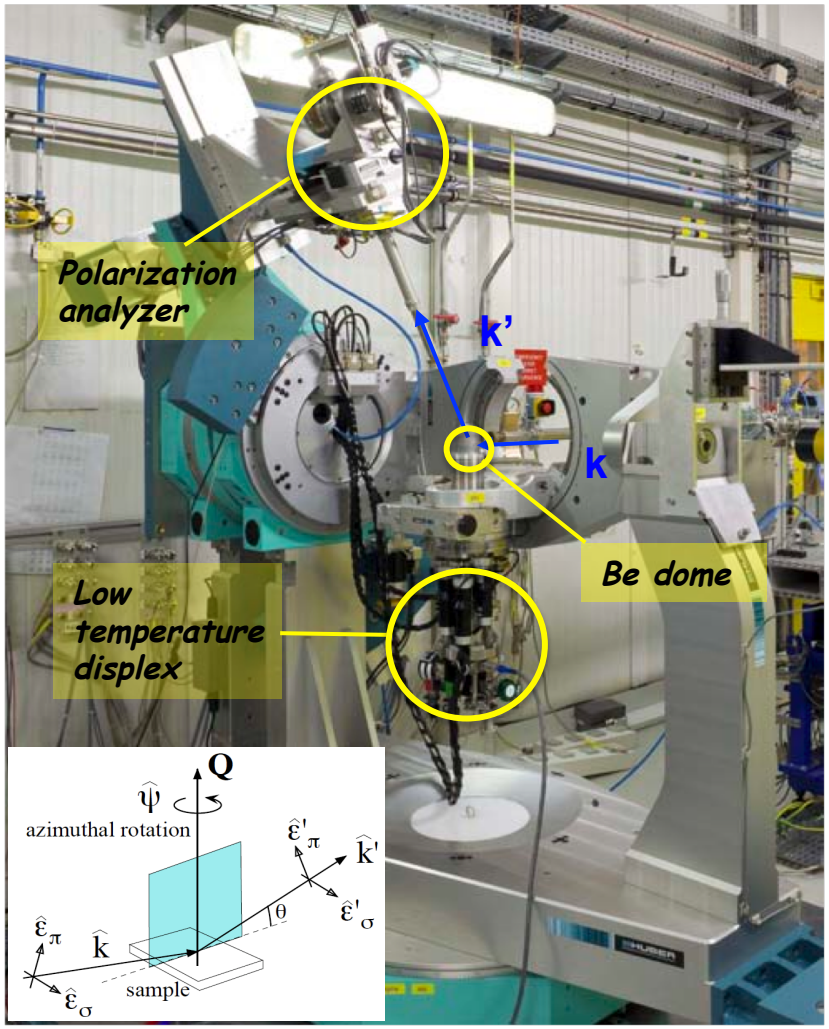

Normal beam diffractometer

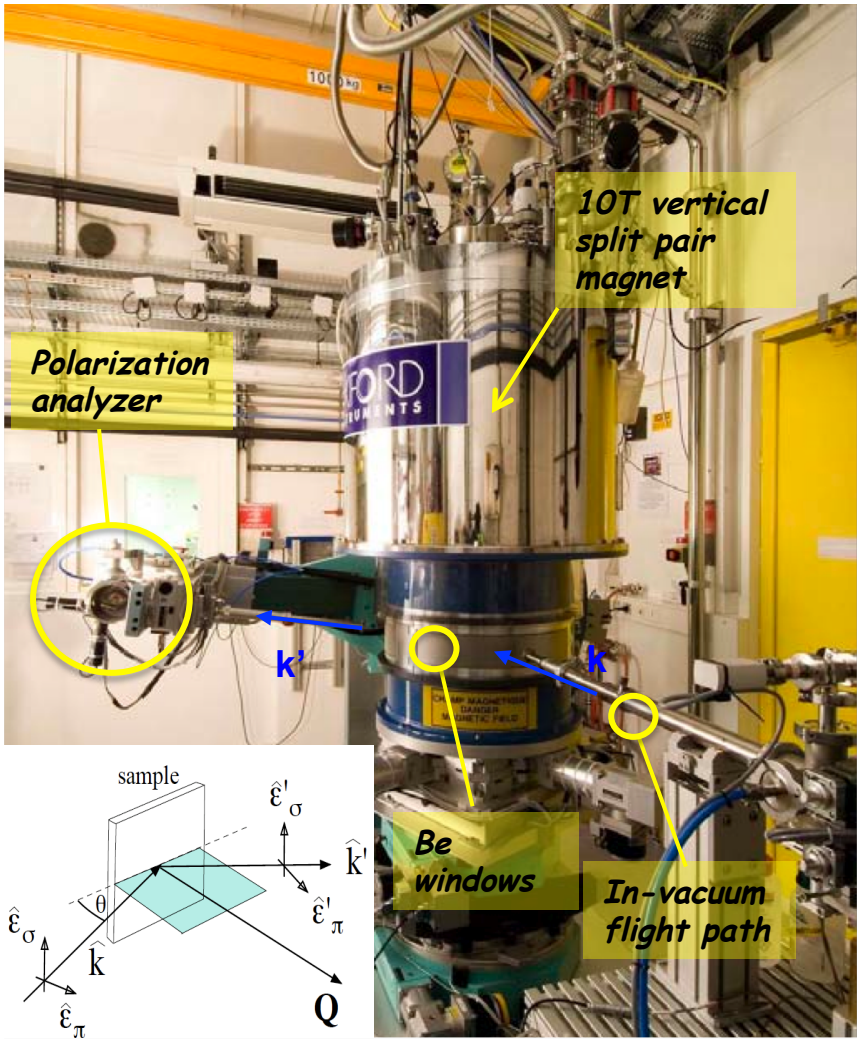

POLARIZATION DEPENDENCE OF nRMXS AMPLITUDES

$$f^{magn.}(\mathbf{Q}) = -i\frac{\hbar\omega_k}{mc^2}\left(\mathbf{L}(\mathbf{Q})\cdot\mathbf{P}_L + \mathbf{S}(\mathbf{Q})\cdot\mathbf{P}_S\right)$$

- *Jones's matrices for nRMXS:*

$$f_{mag}^{non-res} = -i\frac{\hbar\omega}{mc^2}\begin{pmatrix} \sigma\text{–}\sigma' & \pi\text{–}\sigma' \\ M_{\sigma\sigma} & M_{\pi\sigma} \\ M_{\sigma\pi} & M_{\pi\pi} \\ \sigma\text{–}\pi' & \pi\text{–}\pi' \end{pmatrix}$$

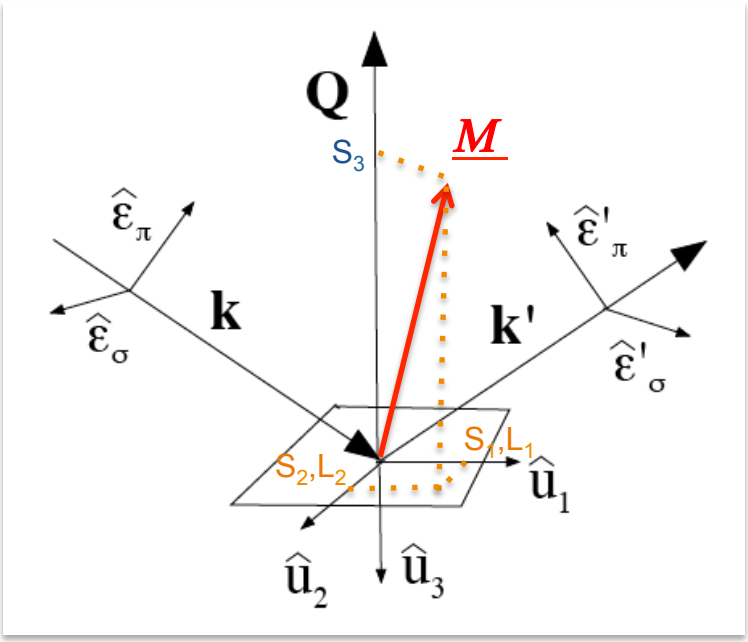

$$\begin{aligned} M_{\sigma\sigma} &= S_2 \sin 2\theta \\ M_{\pi\sigma} &= -2\sin^2\theta\left[(\cos\theta)(L_1+S_1) - S_3\sin\theta\right] \\ M_{\sigma\pi} &= 2\sin^2\theta\left[\cos\theta\,(L_1+S_1) + S_3\sin\theta\right] \\ M_{\pi\pi} &= \sin 2\theta\left[2L_2\sin^2\theta + S_2\right] \end{aligned}$$

$$\begin{aligned} \hat{\mathbf{u}}_1 &= (\hat{\mathbf{k}}+\hat{\mathbf{k}}')/2\cos\theta \\ \hat{\mathbf{u}}_2 &= (\hat{\mathbf{k}}\times\hat{\mathbf{k}}')/\sin 2\theta \\ \hat{\mathbf{u}}_3 &= (\hat{\mathbf{k}}-\hat{\mathbf{k}}')/2\sin\theta \end{aligned}$$

$$S_i = \frac{f_s(Q)\mu_s^i}{g_s\mu_B}$$

$$L_i = \frac{f_l(Q)\mu_l^i}{g_l\mu_B}$$

Fourier components of spin and orbital magnetization densities

AZIMUTHAL LINEAR POLARIMETRY

Charge scattering

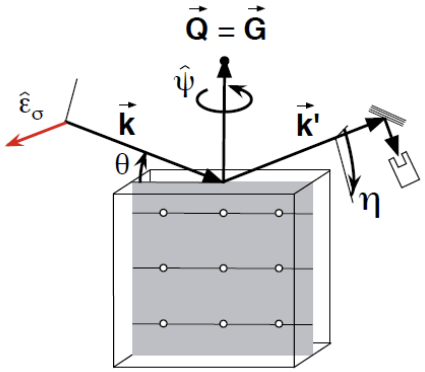

Azimuthal scans

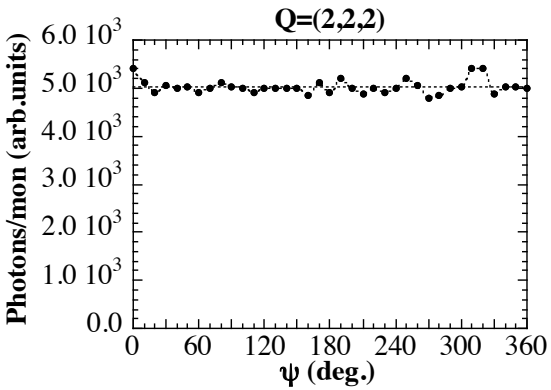

Polarization analysis

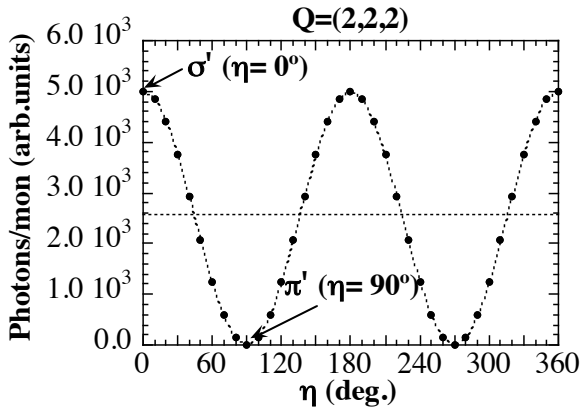

Magnetic scattering

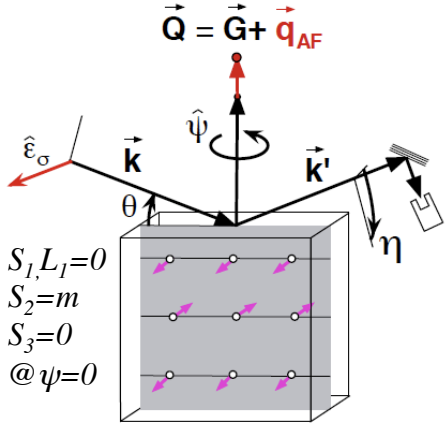

$M_{\sigma\sigma} \sim S_2 \sin 2\theta,$
$M_{\sigma\pi} \sim 2 \sin^2\theta \cos\theta\,(L_1+S_1)$

Azimuthal scans

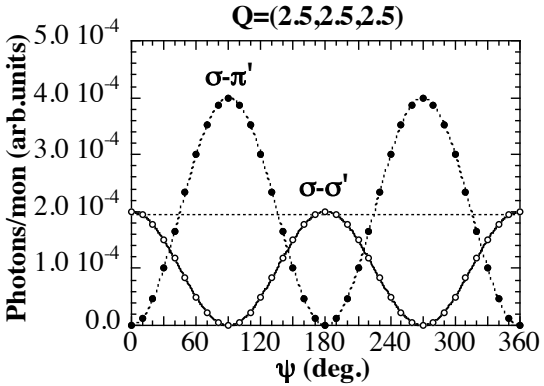

Polarization analysis ψ=90°

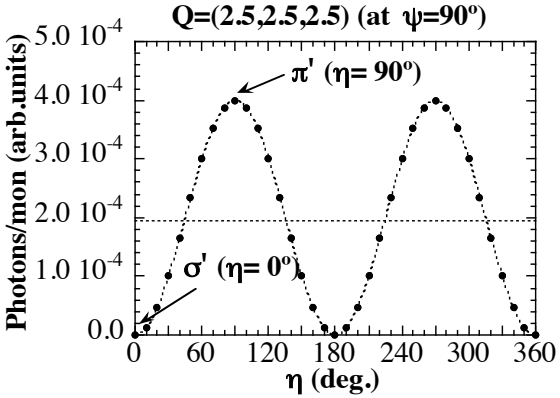

SPIN-ORBIT RATIO IN TRANSITION METAL OXIDES

W. Neubeck at al. J. Phys Chem Sol., 62, 2173 (2001)

Antiferromagnetin transition metal oxides

Polarization dependence of azimuthal scans
Magnetic moment directions
Determination of domain population
L(Q)/S(Q) ratio from polarized intensities

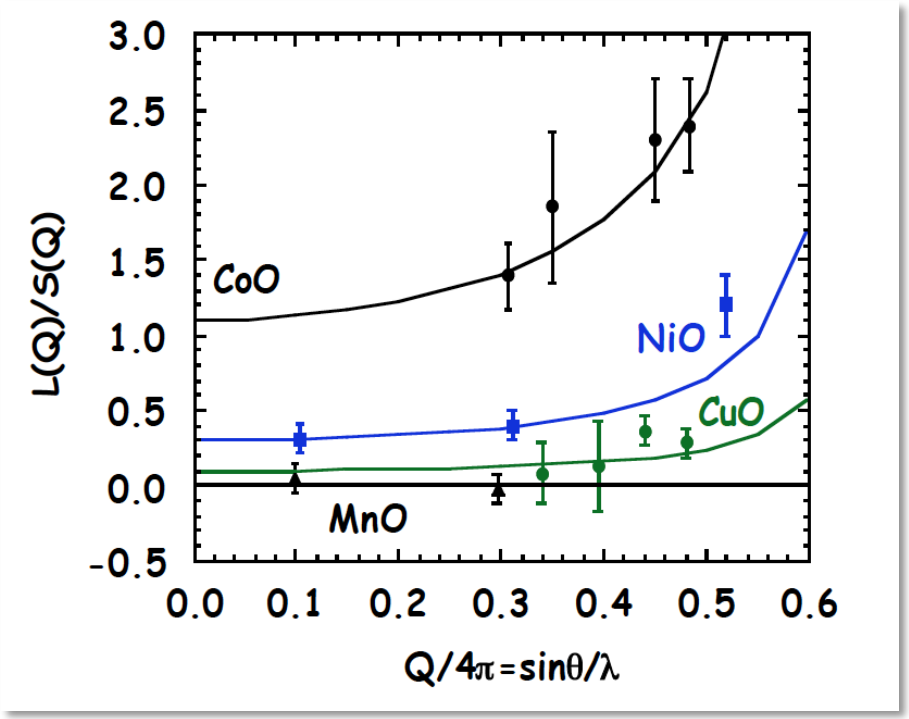

$$P = \frac{I_{\sigma\sigma'} - I_{\sigma\pi}}{I_{\sigma\sigma'} + I_{\sigma\pi}}$$

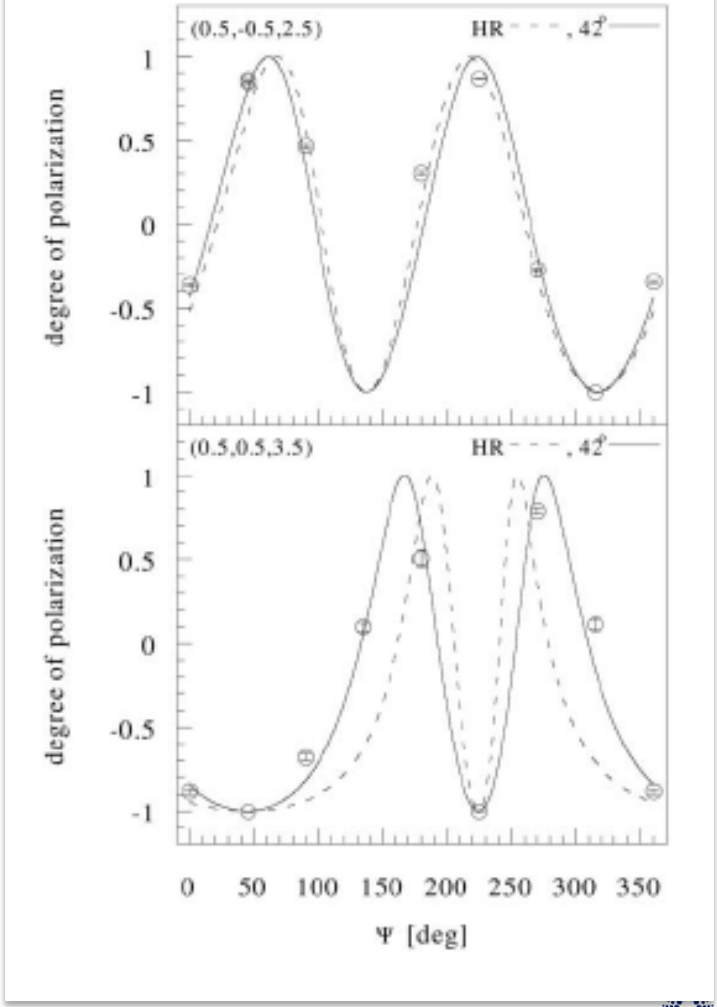

CIRCULAR POLARIMETRY

$I(\eta)=I_0/2\ (1+P_1\sin(2\eta)+P_2\cos(2\eta))$

Stokes-Poincaré parameters:

P_1= linear polarization

P_2= oblique linear polarization

$P_3=1-\sqrt{(P_1^2+P_2^2)}$ = circular polarization

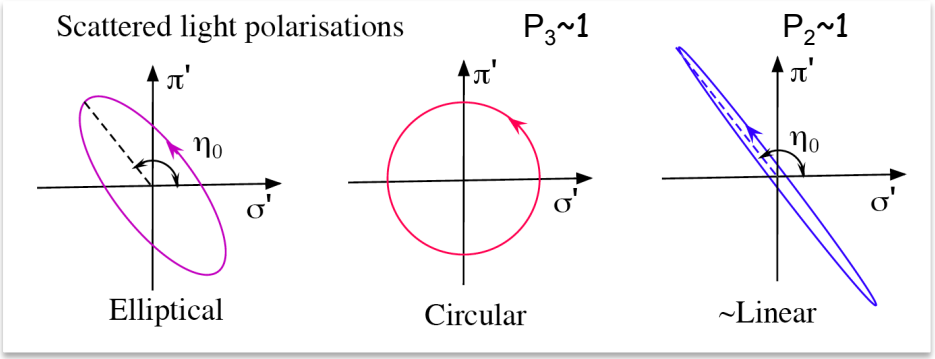

Charge scattering

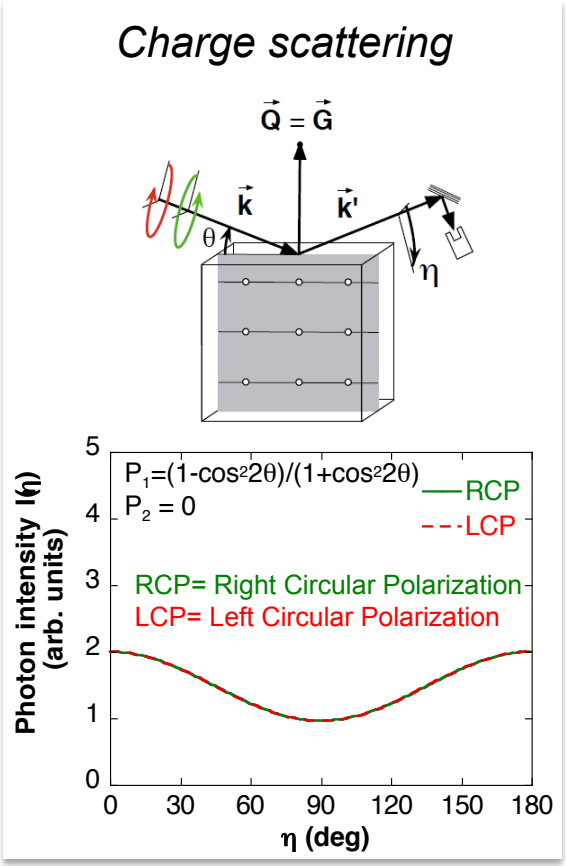

Magnetic scattering

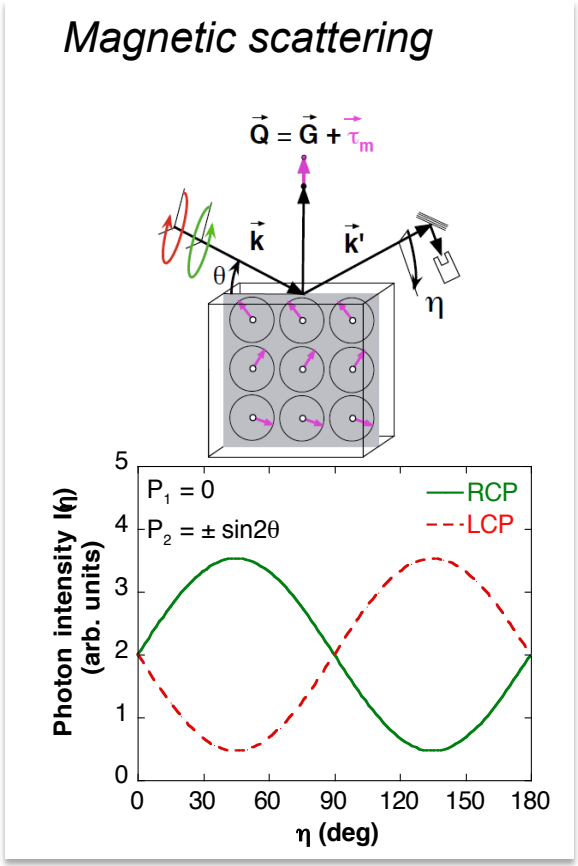

Interference Ch.-Mag.

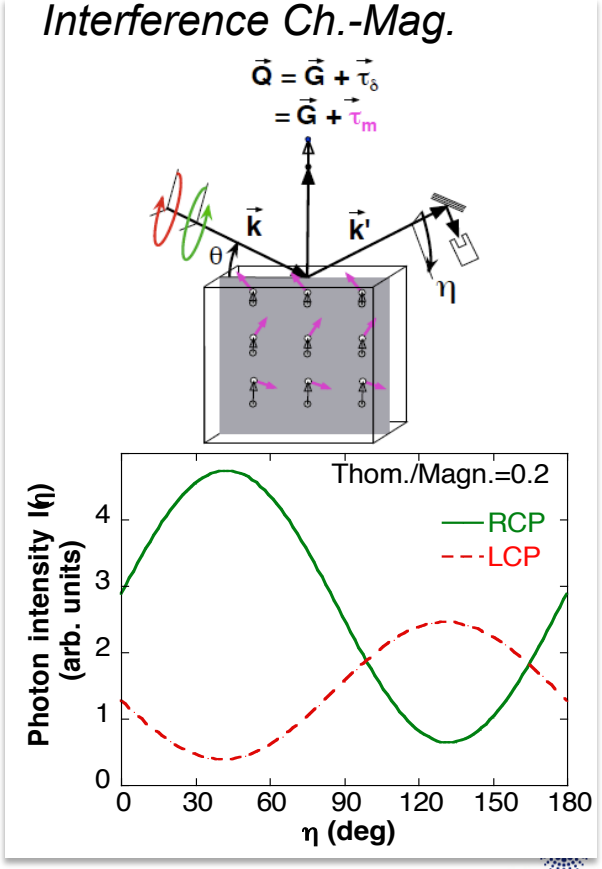

CYCLOIDAL MAGNETISM IN MULTIFERROICS

F. Fabrizi, H.C. Walker, L. Paolasini, F, de Bergevin, A.T. Boothroyd, D. Prabhakaran and D. McMorrow, Phys. Rev. Letters 102 (2009) 237205

- Control of magnetic domain helicity by an electric field
- Complex phase relationships between the Mn and Tb magnetic sublattices
- Complementarities with neutron magnetic scattering

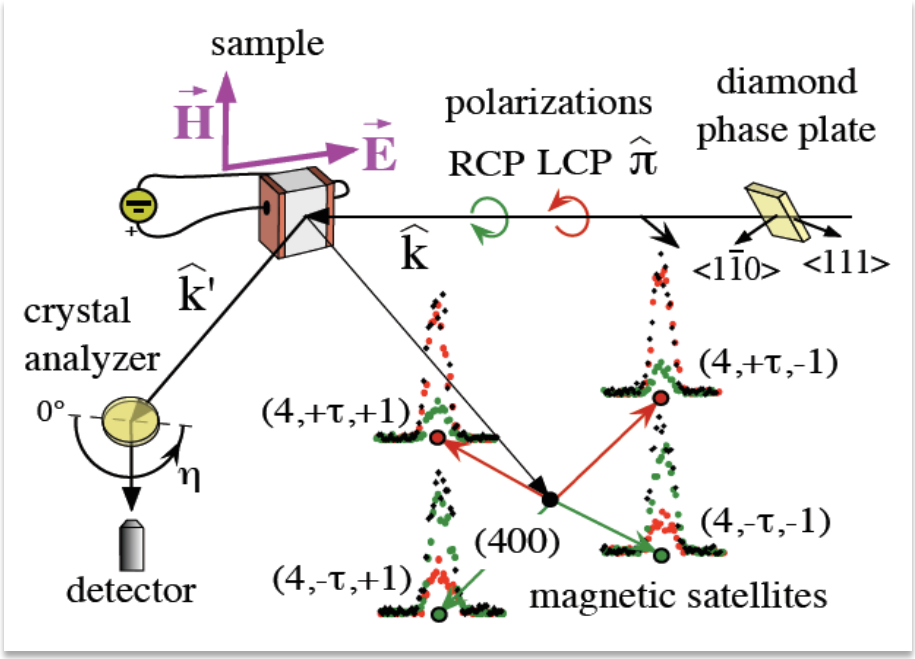

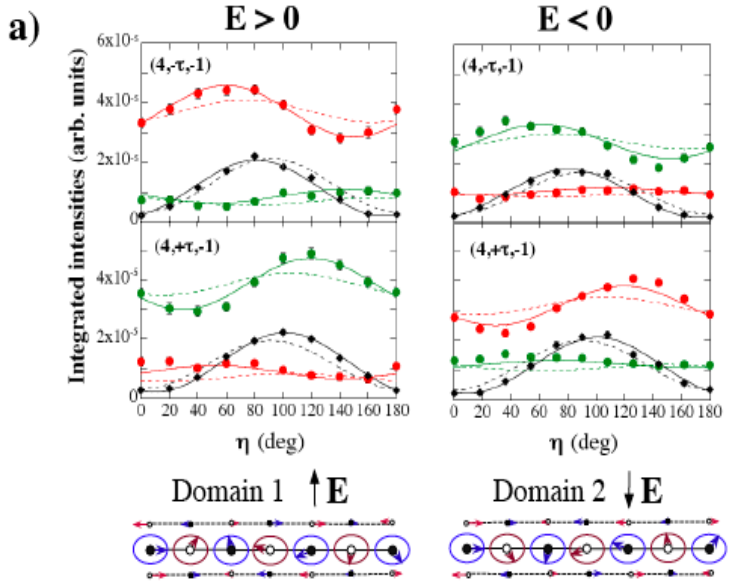

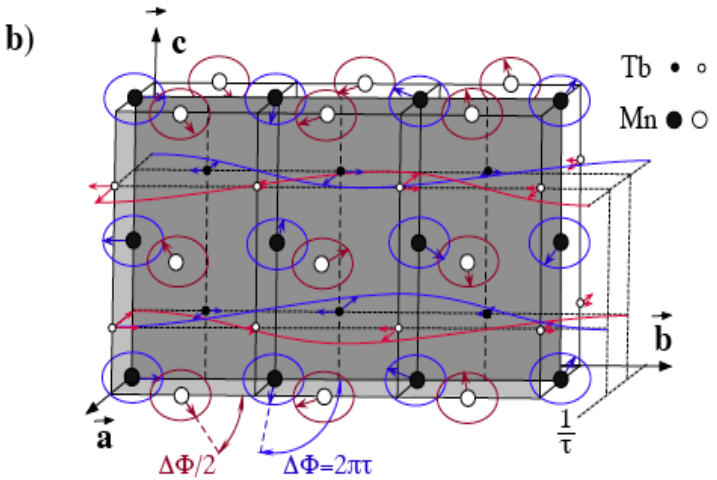

RESONANT X-RAY SCATTERING

$$f^{RXS} \approx -\frac{1}{m}\sum_c \frac{E_g - E_c}{\hbar\omega_k} \cdot \frac{\langle g|\sum_j e^{-i\mathbf{k}'\cdot\mathbf{r}_j}\hat{\epsilon}'^{*}\cdot\mathbf{p}_j|c\rangle\langle c|\sum_j e^{i\mathbf{k}\cdot\mathbf{r}_j}\hat{\epsilon}\cdot\mathbf{p}_j|g\rangle}{E_g - E_c + \hbar\omega_k - i\Gamma_c/2}$$

- Enhancement of scattering amplitude near absorption edge
- Excitation of a inner-shell electron into an empty valence state
- Sensitivity to the local degeneration of valence-electron states

- Local symmetries of bound electrons
- Tensorial structure factor
- Forbidden lattice reflections
- Polarization effects (links with magneto-optics)
- Mixing diffraction and atomic spectroscopy

E1 = Electric dipole transitions (L=1)
E2 = Electric quadrupole transitions (L=2)

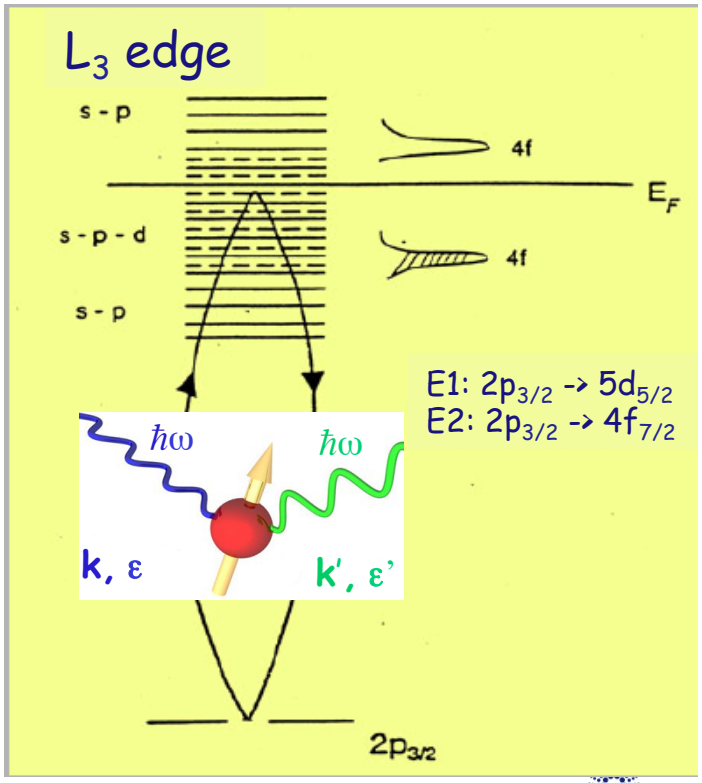

RESONANT MAGNETIC X-RAY SCATTERING AMPLITUDES

- *Expansion of spatial part of vector potential in spherical harmonics Y_{LM}*
- *Spherical symmetry SU(2) broken by an axial vector*
- *Cubic and centro-symmetric local symmetries*

$$f^{RXS} = \sum_{L,M} F_{LM}(\hbar\omega_k) \left[\hat{\epsilon}' \cdot \mathbf{Y}^{(e)}_{L,M}(\hat{\mathbf{k}}') \mathbf{Y}^{*(e)}_{L,M}(\hat{\mathbf{k}}) \cdot \hat{\epsilon}\right]$$

Resonant strength

Geometrical and polarization dependence

$$F_{LM}(\hbar\omega_k) = \sum_{a,c} p_a p_a(c) \frac{E_a - E_c}{\hbar\omega_k} \frac{\Gamma_x(aMc; EL)/\Gamma_c}{x + i} \qquad x = \frac{E_a - E_c + \hbar\omega_k}{\Gamma_c/2}$$

$$\Gamma_x(aMc; EL) = 2 * \frac{(4\pi)^2}{((2L+1)!!)^2} \frac{L+1}{L} mc^2 \left|\left\langle a \left| (kr)^L Y^*_{LM}(\hat{\mathbf{r}}_j) \right| c \right\rangle\right|^2$$

Matrix elements

L=1 => Electric dipole E1
L=2 => Electric quadrupole E2

RXS ABSORPTION EDGES: ELEMENT AND SHELL SELECTIVITY

Series	Abs. edge	Energy (keV)	λ (Å)	Shells	Type	Resonant amplitude
3d	*$L_{2,3}$*	*0.4–1.0*	*12–30*	*2p→3d*	*E1*	*≈100*
	K	4.5–9.5	1.3–2.7	1s→4p	E1	≈0.02
				1s→3d	E2	≈0.01
5d	**$L_{2,3}$**	5.4–14	0.9–2.2	*2p→5d*	E1	≈1-10
4f	**$L_{2,3}$**	5.7–10.3	1.2–2.2	2p→5d	E1	≈0.10
				2p→4f	E2	≈0.05
	$M_{4,5}$	*0.9–1.6*	*7.7–13.8*	*2d→4f*	*E1*	*≈100-300*
5f	**$L_{2,3}$**	17–21	0.6–0.7	2p→6d	E1	≈0.05
				2p→4f	E2	≈0.01
	$M_{4,5}$	3.5–4.5	2.7–6	3d→5f	E1	≈10.0

RESONANT ENHANCEMENT STRENGTH (E1)

Matrix elements of electric dipole transition E1

$$\langle n|\boldsymbol{r}|g\rangle \propto \int_0^\infty r^2\,dr\,\underbrace{R_{nl}(r)}_{\text{core electrons}}\,r\,\underbrace{R_{n'l'}(r)}_{\text{valence electrons}}$$

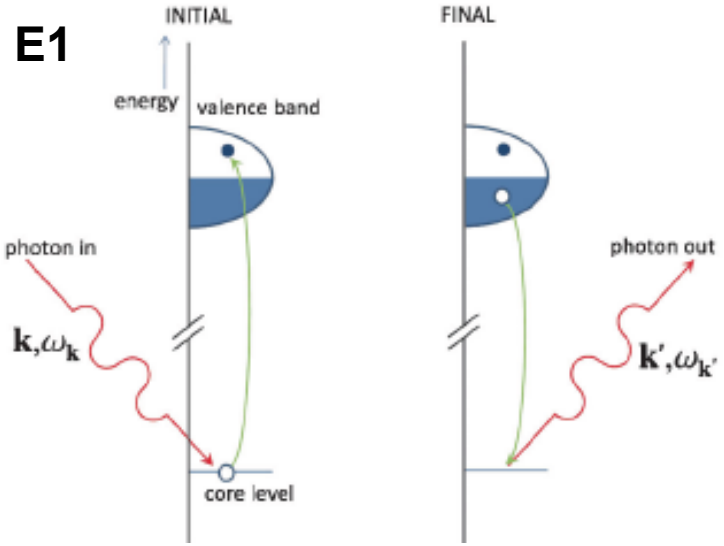

Large resonance = large overlap between the core and valence electron radial wavefunctions.

Transition Metals 3d	L edges, 2p->3d c. 1 keV	Strong
Transition Metals 5d	L edges, 2p->5d c. 10 keV	medium
Rare-Earths 4f,5d	L edges, 2p->5d c. 10 keV	Weak
Rare-Earths 4f,5d	M edges, 3d->4f c. 1 keV	Strong
Actinides 5f	M edges, 3d->5f c. 3 keV	Strong

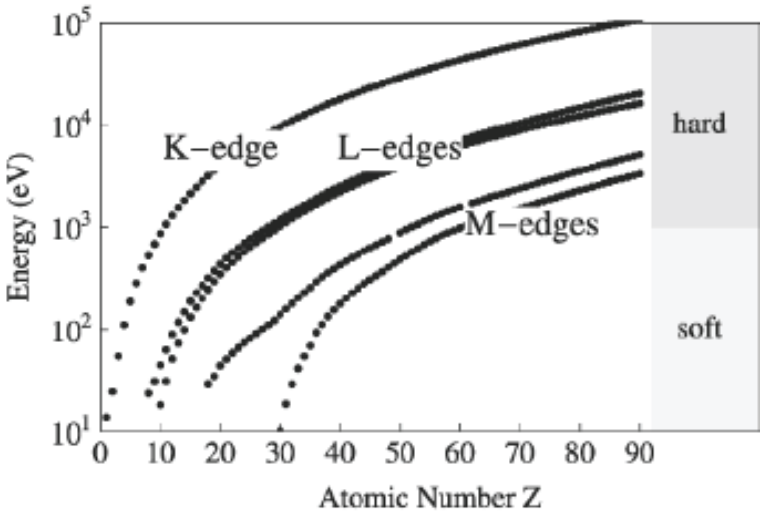

E1 ELECTRIC DIPOLE TRANSITIONS

- Dominant terms in RXS scattering amplitudes

$$f_{E1}^{res} = \left[\hat{\epsilon}' \cdot \hat{\epsilon} F_{E1}^{(0)} - i(\hat{\epsilon}' \times \hat{\epsilon}) \cdot \mathbf{z}_n F_{E1}^{(1)} + (\hat{\epsilon}' \cdot \mathbf{z}_n)(\hat{\epsilon} \cdot \mathbf{z}_n) F_{E1}^{(2)}\right]$$

$$F_{E1}^{(0)} = \frac{3}{16\pi}[F_{11} + F_{1-1}] \quad \longleftarrow \textit{Charge scattering}$$

$$F_{E1}^{(1)} = \frac{3}{16\pi}[F_{11} - F_{1-1}] \quad \longleftarrow \textit{Magnetic dipole}$$

$$F_{E1}^{(2)} = \frac{3}{16\pi}[2F_{10} - F_{11} - F_{1-1}] \quad \longleftarrow \textit{Electric quadrupole}$$

- Polarization dependence for the magnetic dipole:
  - Horizonthal scattering geometry
  - π-incident polarization

ε_π-ε'_σ $\quad z_1 \cos\theta + z_3 \sin\theta$

ε_π-ε'_π $\quad -z_2 \sin 2\theta$

z_i magnetic dipole component along u_i

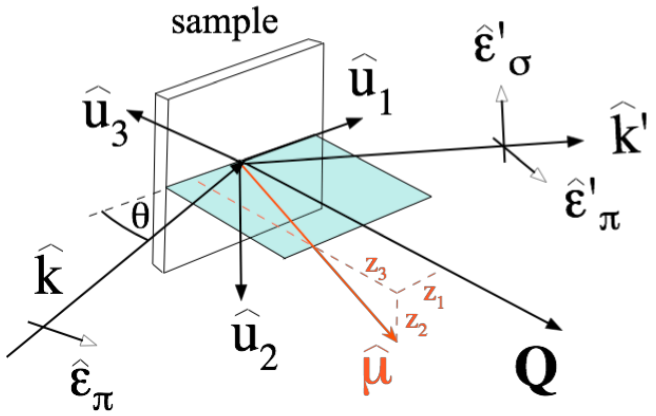

ELECTRIC DIPOLE TRANSITIONS

- Dominant terms in RXS amplitudes at M-edges of Actinides:

$$f_{E1}^{res} = \left[\hat{\epsilon}' \cdot \hat{\epsilon} F_{E1}^{(0)} - i(\hat{\epsilon}' \times \hat{\epsilon}) \cdot \mathbf{z}_n F_{E1}^{(1)} + (\hat{\epsilon}' \cdot \mathbf{z}_n)(\hat{\epsilon} \cdot \mathbf{z}_n) F_{E1}^{(2)}\right]$$

$$F_{E1}^{(0)} = \frac{3}{16\pi}[F_{11} + F_{1-1}] \quad \longleftarrow \textit{Charge scattering}$$

$$F_{E1}^{(1)} = \frac{3}{16\pi}[F_{11} - F_{1-1}] \quad \longleftarrow \textit{Magnetic dipole}$$

$$F_{E1}^{(2)} = \frac{3}{16\pi}[2F_{10} - F_{11} - F_{1-1}] \quad \longleftarrow \textit{Electric quadrupole}$$

- Polarization dependence for the magnetic dipole:
  - Horizonthal scattering geometry
  - π-incident polarization

ε_π-ε'_σ	0
ε_π-ε'_π	$-z_2 \sin 2\theta$

z_2 magnetic dipole component along u_2

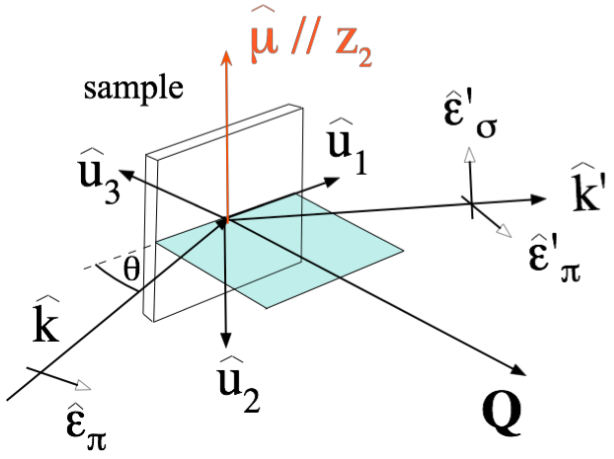

ELECTRIC DIPOLE TRANSITIONS

- Dominant terms in RXS amplitudes at M-edges of Actinides:

$$f_{E1}^{res} = \left[\hat{\epsilon}' \cdot \hat{\epsilon} F_{E1}^{(0)} - i(\hat{\epsilon}' \times \hat{\epsilon}) \cdot \mathbf{z}_n F_{E1}^{(1)} + (\hat{\epsilon}' \cdot \mathbf{z}_n)(\hat{\epsilon} \cdot \mathbf{z}_n) F_{E1}^{(2)}\right]$$

$$F_{E1}^{(0)} = \frac{3}{16\pi}[F_{11} + F_{1-1}] \quad \longleftarrow \textit{Charge scattering}$$

$$F_{E1}^{(1)} = \frac{3}{16\pi}[F_{11} - F_{1-1}] \quad \longleftarrow \textit{Magnetic dipole}$$

$$F_{E1}^{(2)} = \frac{3}{16\pi}[2F_{10} - F_{11} - F_{1-1}] \quad \longleftarrow \textit{Electric quadrupole}$$

- Polarization dependence for the magnetic dipole:
  - Horizonthal scattering geometry
  - π-incident polarization

ε_π-ε'_σ	$z_3 \sin\theta$
ε_π-ε'_π	0

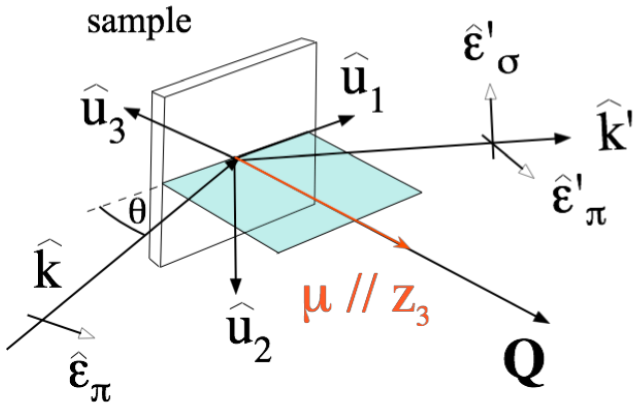

z_3 magnetic dipole component along u_3

RMXS AT M-EDGES OF ACTINIDES

Resonant magnetic scattering in $(U_{0.5}Np_{0.5})Ru_2Si_2$ solid solution
E. Lidstrom et al., Phys. Rev. B 61, 1375 (2000)

Actinide Sample:
mounted on 2x2 mm² Ge(111) wafer
volume 0.1 mm³, **30 μg Np**
Element selectivity and sublattice magnetization
Np and U at $M_{4,5}$ edges

Branching ratios between M_4-M_5 edges
Electronic ground state
Exchange and spin-orbit coupling

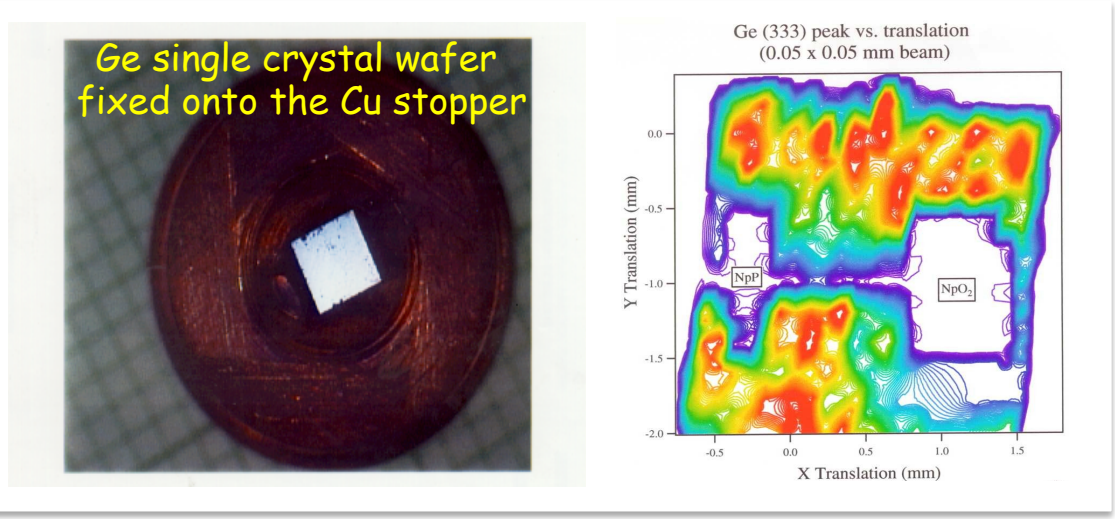

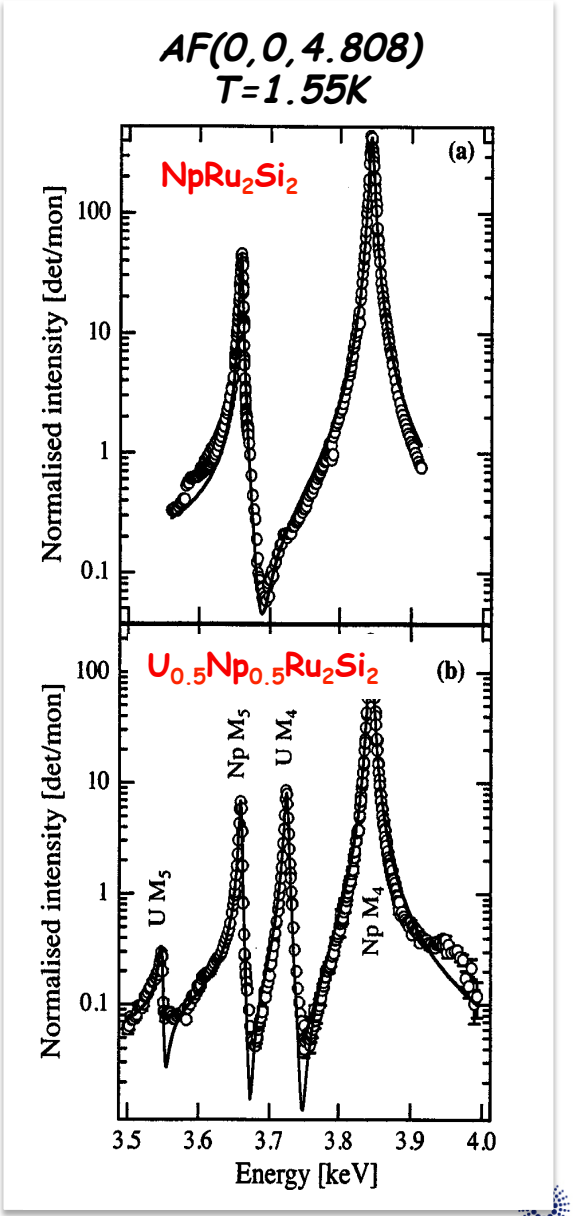

INTERPLAY BETWEEN ORBITAL AND MAGNETIC ORDERING

Interplay between orbital and magnetic ordering in $KCuF_3$
R. Caciuffo, et al., Phys. Rev. B 63 (2002) 174425; ibid. L. Paolasini, Phys. Rev. Letters 88 (2002) 106403.

Scientific background

- Mott-Hubbard insulator
- Model system for orbital ordering

Experimental results

- Orbital and AF order strictly related.
- OO of $d_{y^2-z^2}$ - $d_{x^2-z^2}$ type with q_{OO}=<111>.
- ATS due to the difference in the $2p_{x(y)}$ DOS (Jahn-Teller distortion)

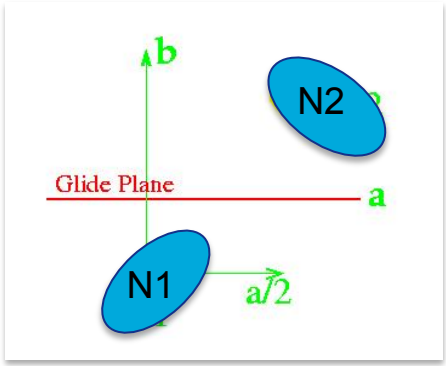

Violation of the extinction rules

$f(N_1)+f(N_2)\exp[i\pi h]$

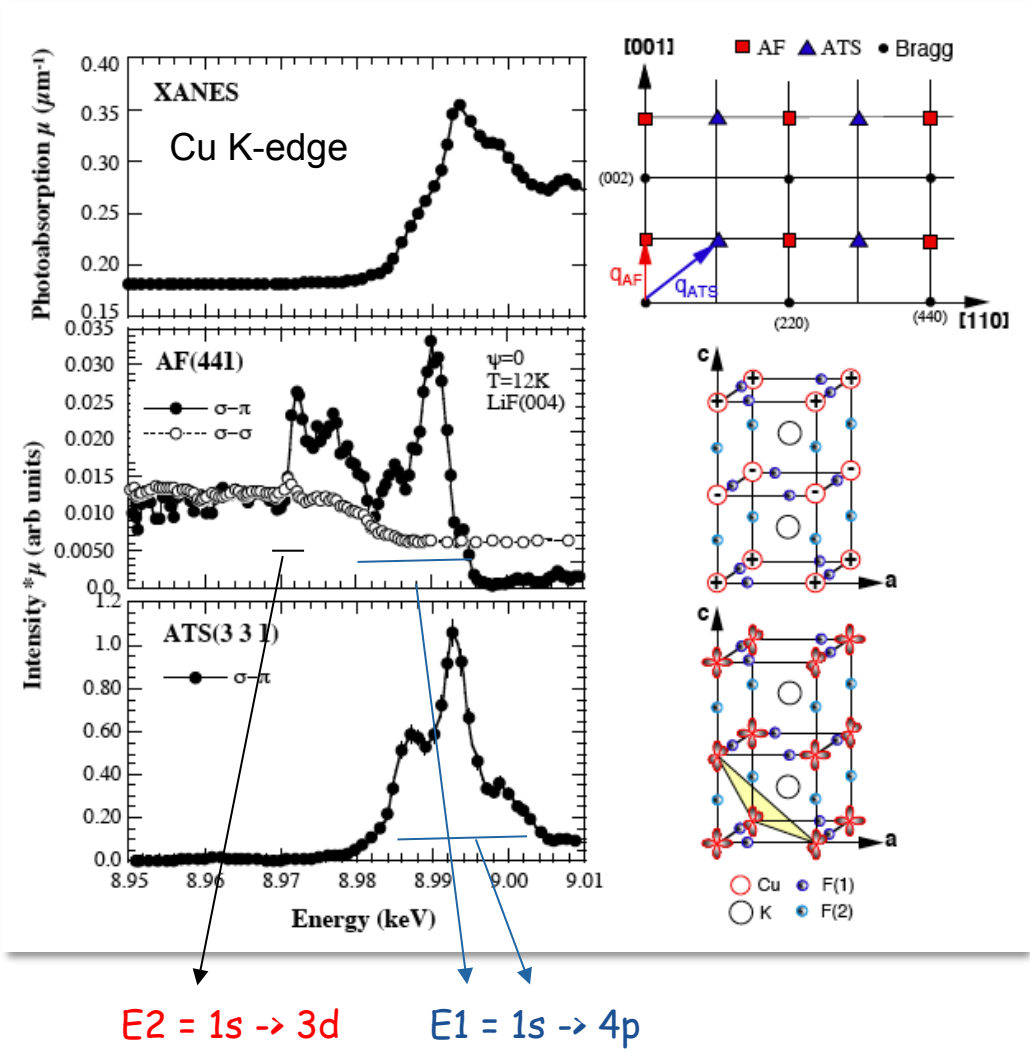

CHARGE ORDERING IN $NdNiO_3$ THIN FILM

Direct observation of charge order in epitaxial $NdNiO_3$ films
Staub U. et al., Phys. Rev. Letters 88 (2002) 126402.

- Prototype of bandwidth-controlled metal-insulator
- Metal/insulator transition T_{MI}=150-170K

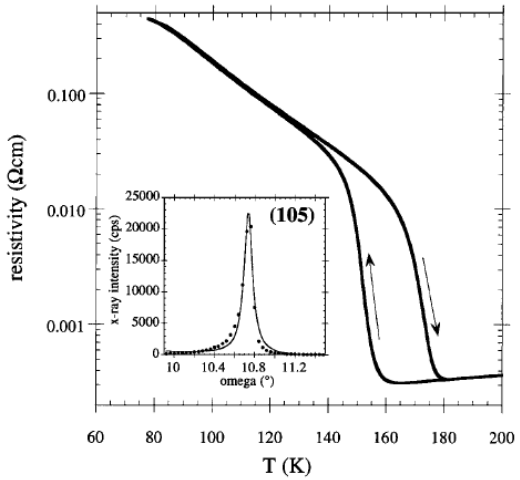

Experimental results

- Strong enhancement of RXS at Ni K-edge on the forbidden charge reflection (105)
- ATS due to a charge dis-proportionation at Ni^{3+} site

$Nd^{3\pm\delta}$ where δ~0.45±0.04

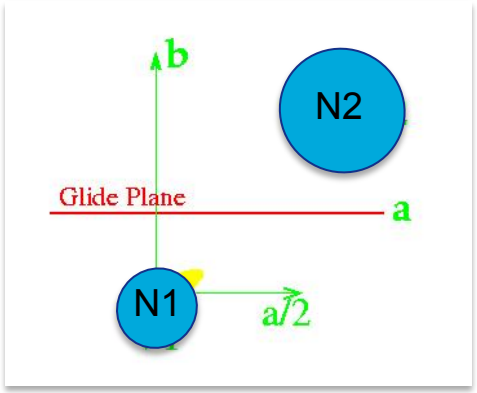

Violation of the extinction rules

$f(N_1) \neq f(N_2)$

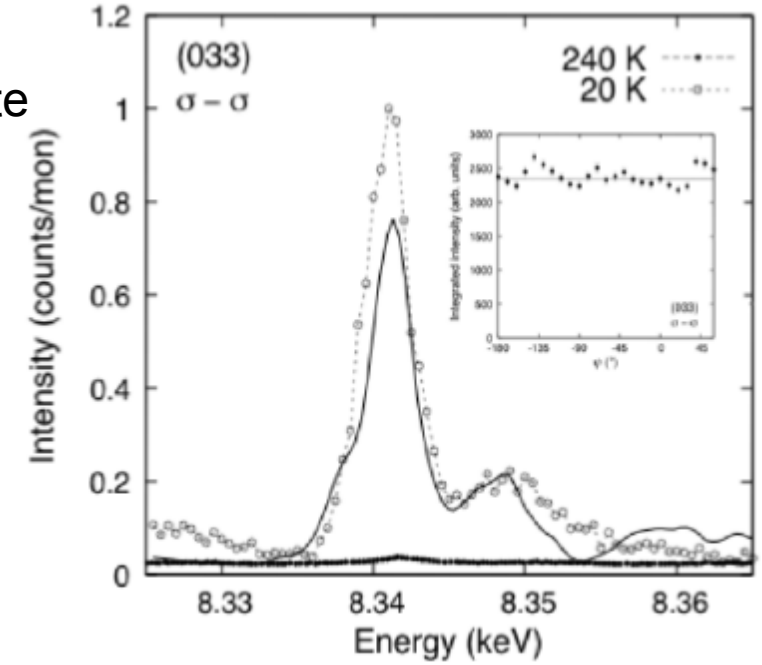

RXS AND HIGH ORDER MULTIPOLE EXPANSION

Dubovik, V.M. & Tugushev, V.V., Physics Reports 187, 145-202 (1990)
L. Paolasini, F. de Bergevin C.R. Physique 9, 550 (2008)
Di Matteo, J. Phys. D: Appl. Phys. 45 163001 (2012).

Product of irreducible spherical tensors X_q and F_q.
The rank q depends on the order of multipole in the EM field expansion:

$$f_j^{RXS} = \sum (-1)^q X_{-q}^{(p)} F_q^{(p)}(j;\omega)$$

Tensor	rank	$\hat{T}$	$\hat{P}$	Type	Multipole
$F^{(0)}(E1-E1)$	0	+	+	charge	monopole
$F^{(0)}(E2-E2)$	0	+	+	charge	monopole
$F^{(1)}(E1-E1)$	1	-	+	magnetic	dipole
$F^{(1)}(E2-E2)$	1	-	+	magnetic	dipole
$F^{(1+)}(E1-E2)$	1	+	-	electric	dipole
$F^{(1-)}(E1-E2)$	1	-	-	polar toroidal	dipole
$F^{(2)}(E1-E1)$	2	+	+	electric	quadrupole
$F^{(2)}(E2-E2)$	2	+	+	electric	quadrupole
$F^{(2+)}(E1-E2)$	2	+	-	axial toroidal	quadrupole
$F^{(2-)}(E1-E2)$	2	-	-	magnetic	quadrupole
$F^{(3)}(E2-E2)$	3	-	+	magnetic	octupole
$F^{(3+)}(E1-E2)$	3	+	-	electric	octupole
$F^{(3-)}(E1-E2)$	3	-	-	polar toroidal	octupole
$F^{(4)}(E2-E2)$	4	+	+	electric	hexadecapole

$P^{+/-}T^{+}$ Electric/charge

$P^{+}T^{-}$ Magnetic

$P^{-}T^{-}$ Magneto-electric

MULTIPOLAR ORDERED STATE IN V_2O_3

Experiments:

L. Paolasini, Phys.Rev.Lett. (1999); *ibid* L. Paolasini, et. al J. Electron Spectrosc. Relat. Phenom. 120, 1 (2001)

J. Fernandez-Rodrıguez, V. Scagnoli, C. Mazzoli, F. Fabrizi, S.W. Lovesey, J. A. Blanco, D.S. Sivia, K.S. Knight, F. de Bergevin, and L. Paolasini, Phys. Rev. B **81** (2010) 085107.

Theory:

S. Di Matteo, Y. Joly, A. Bombardi, L. Paolasini, F.de Bergevin, and C.R. Natoli, Phys. Rev. Lett. 91, 257402 (2003)

S. Loversey, J. Fernandez-Rodriguez, J.A. Blanco, D.S. Sivia, K.S. Knight, L. Paolasini, Phys. Rev. B **75** (2007) 014409

ATS
$(00.l)_H$ l_H=3(2n+1)

Electric octupole and hexadecapole
F^3(E1-E2)+F^4(E2-E2)

ATS
$(h0.-h)_m$ h_m=2n+1

Electric quadrupole
F^2(E1-E1)
(dominant contribution)

AF reflections
k_m+l_m=even and h_m=even

Magnetic dipole and magnetic quadrupole
F^1(E1-E1)+$F^{2\text{-}}$(E2-E2)

Special reflections
k_m+l_m=even and h_m=odd

Polar toroidals and magnetic quadrupole
$F^{(1,3)\text{-}}$(E1-E2) and F^2(E2-E2)

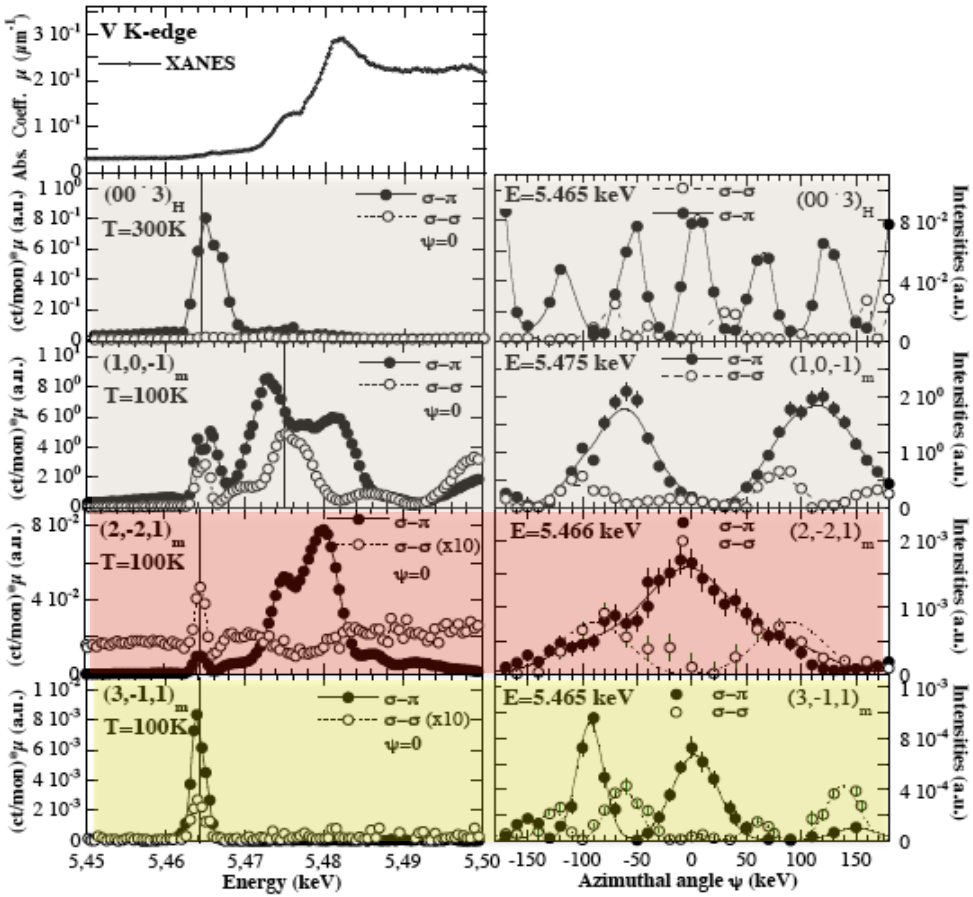

RESONANT INELASTIC X-RAY SCATTERING - RIXS

Probe elementary excitations in complex materials by measuring their energy, momentum, and polarization dependence.

- Element and electron shell specific
- Momentum and energy resolved
- Probes excitation spectrum from meV to eV
- Large resonant enhancements possible
- Small micron sized samples can be studied
- Single magnon excitations can be measured

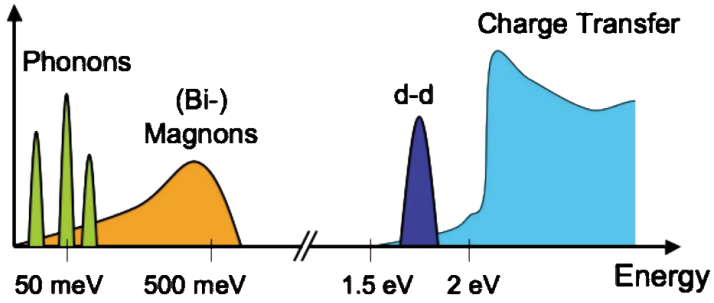

Experimental advances

- Aggressive improvement of energy resolution, but still high with respect neutron inelastic energies
- Hard x-rays edges limited by resonance enhancement
- Future perspectives for advances X-FEL

RESONANT INELASTIC X-RAYS SCATTERING

Theoretical framework

Ament et al., Rev. Mod. Phys. ***83***, *705 (2011)*

$$w = \frac{2\pi}{\hbar} \sum_{\mathrm{f}} |\langle \mathrm{f}|\mathcal{H}'|g\rangle + \sum_{n} \frac{\langle \mathrm{f}|\mathcal{H}'|n\rangle\langle \mathrm{n}|\mathcal{H}'|g\rangle}{E_g - E_n}|^2 \delta(E_{\mathrm{f}} - E_g)$$

$$E_g = E_{\mathrm{g}} + \hbar\omega_{\mathbf{k}} \qquad E_{\mathrm{f}} = E_f + \hbar\omega_{\mathbf{k}'}$$

When $E_g \sim E_n$ *the second order dominate and the interaction hamiltonian H' leading term is:*

$$\mathcal{H}' = \frac{e\mathbf{A}\cdot\mathbf{p}}{m}$$ Linear term in vector potential

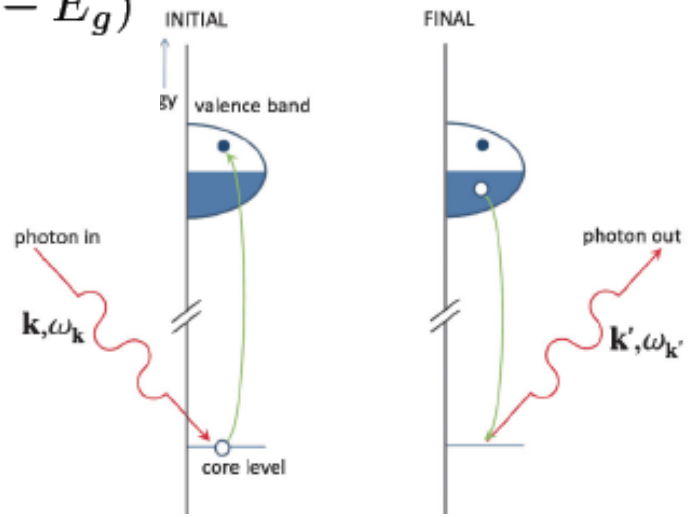

Kramer-Heisenberg RIXS cross section:

$$I(\omega, \mathbf{k}, \mathbf{k}', \epsilon, \epsilon', \omega_{\mathbf{k}}, \omega_{\mathbf{k}'}) = r_0^2 m^2 \omega_{\mathbf{k}}^4 \sum |\mathcal{F}_{fg}(\mathbf{k}, \mathbf{k}', \epsilon, \epsilon', \omega_{\mathbf{k}}, \omega_{\mathbf{k}'})|^2 \delta(E_{\mathrm{g}} - E_f + \hbar\omega)$$

$$\mathcal{F}_{fg}(\mathbf{k}, \mathbf{k}', \epsilon, \epsilon', \omega_{\mathbf{k}}, \omega_{\mathbf{k}'}) = \sum_{n} \frac{\langle f|\mathcal{D}'|n\rangle\langle n|\mathcal{D}|\mathrm{g}\rangle}{E_{\mathrm{g}} + \hbar\omega_{\mathbf{k}} - E_n - i\Gamma_n}$$ RIXS scattering amplitude

$$\mathcal{D} = \epsilon \cdot \mathbf{D} \qquad \langle n|\mathbf{D}|\mathrm{g}\rangle = \sum_{i=1}^{N} e^{i\mathbf{k}\cdot\mathbf{R}_i} \langle n|\mathbf{r}|\mathrm{g}\rangle$$ Electric dipole operator

RIXS SPECTROMETER ID20 AT ESRF

Courtesy M. Moretti

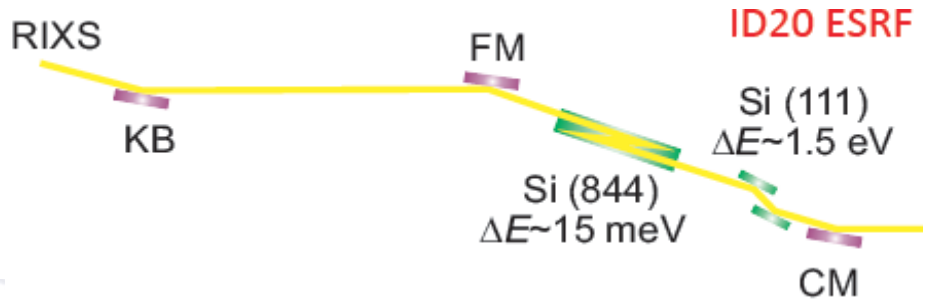

5 bent or diced analysers
ΔE down to 25 meV
High flux and/or several **q**'s

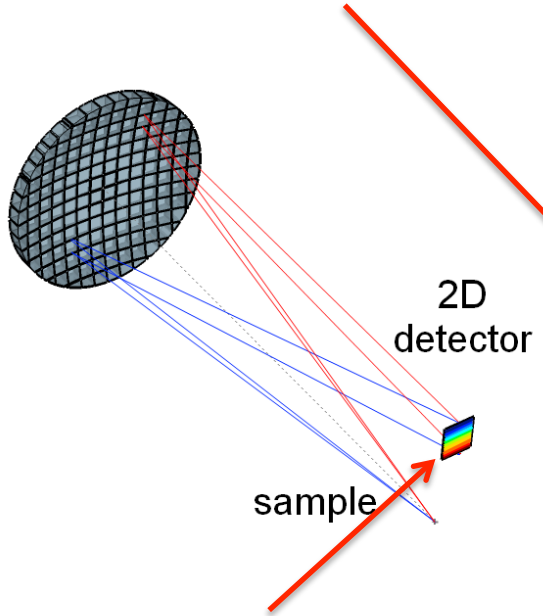

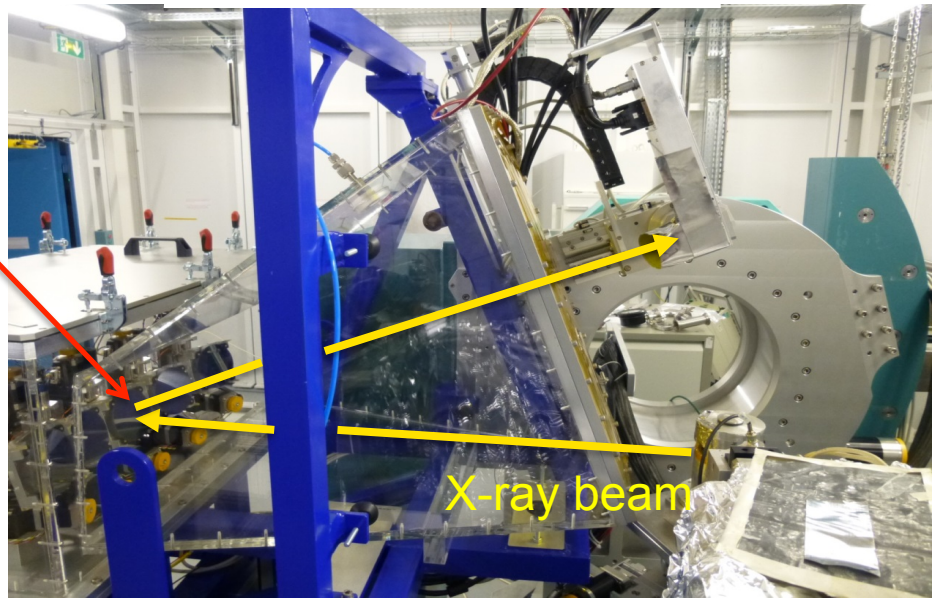

1x5 Maxipix Detectors
55 μm pixel size
Energy compensation algorithm
Background removal

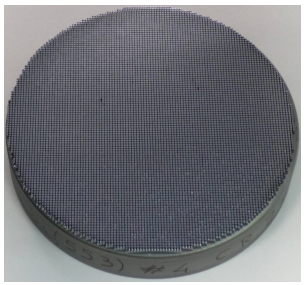

Diced Analyzers
very high energy resolution
cube size 0.8 mm x 0.8 mm x 3 mm
Curvature radius 1, 2, 6.5 m
Energy compensation algorithm

OBSERVATION OF SINGLE MAGNONS BY RIXS IN La_2CuO_4

RIXS on at Cu L3 edge (930 eV)

Braicovich et al. (2010)

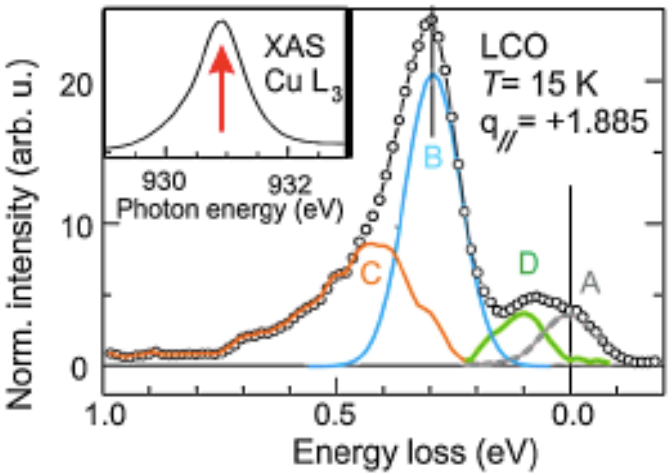

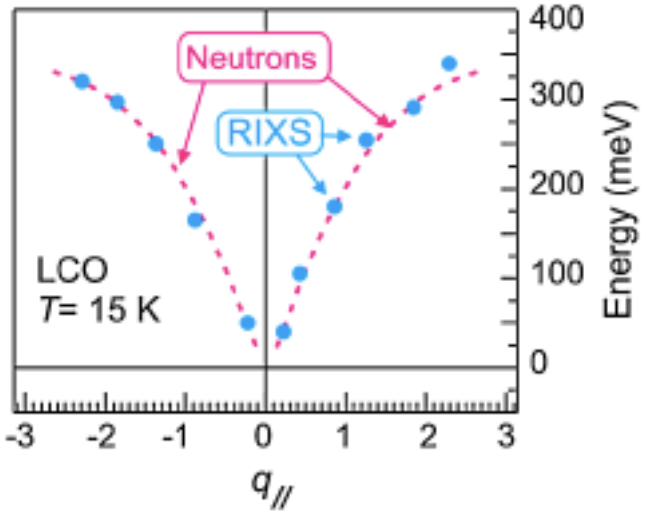

Theoretical interpretation based on Hubbard model

Jia et al. Nat. Comm (2013)

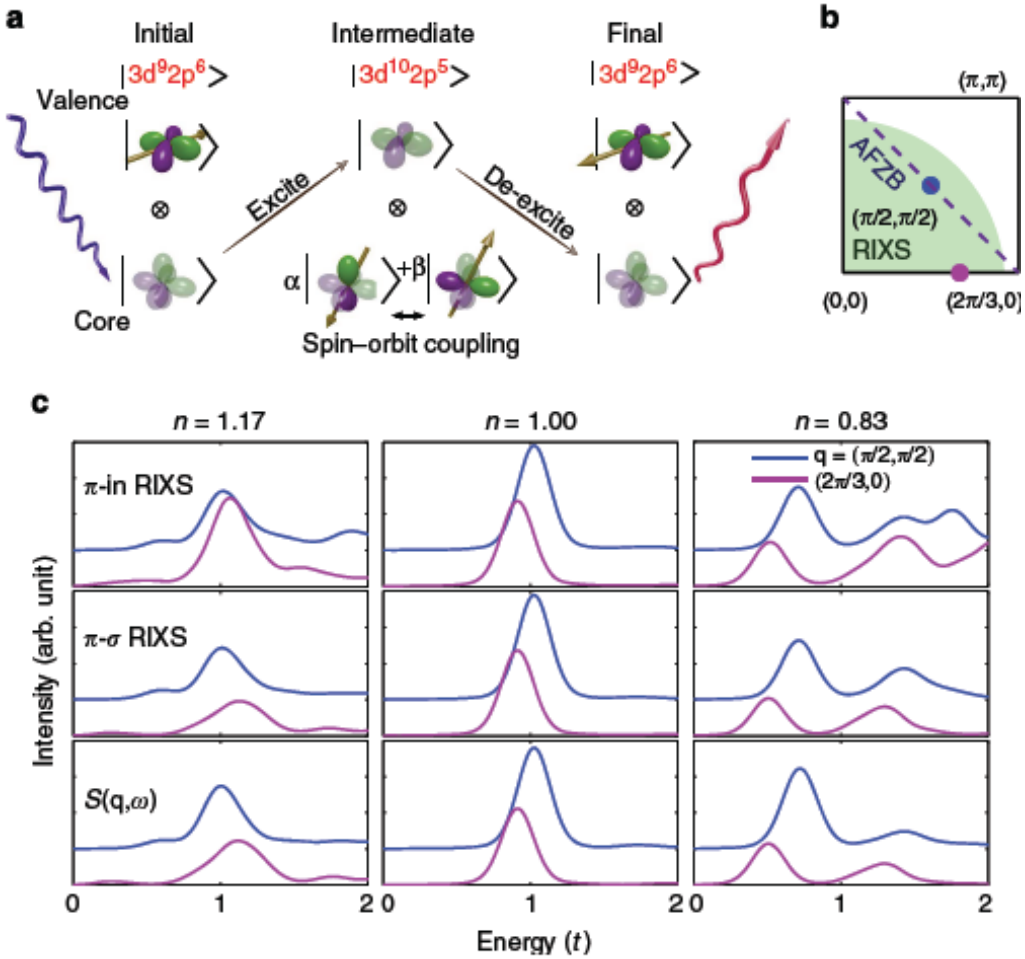

Courtesy D. McMorrow

Mott-Hubbard-Heisenberg paradigm

- Mott-Hubbard insulating state arises from electron-electron interactions
- Mott-Hubbard Metal-insulator transition independent of magnetic order
- Lowest energy spin physics described by isotropic Heisenberg Hamiltonian

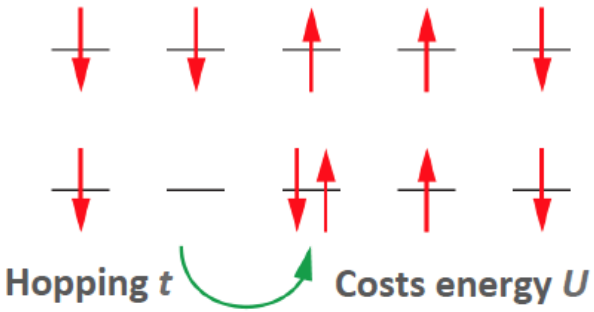

$$\mathcal{H}_{Hubbard} = \mathcal{H}_{kinetic}(t) + \mathcal{H}_{repulsion}(U)$$

$$\mathcal{H} = J \sum_{<ij>} \mathbf{S}_i \cdot \mathbf{S}_j \qquad J = \frac{4t^2}{U}$$

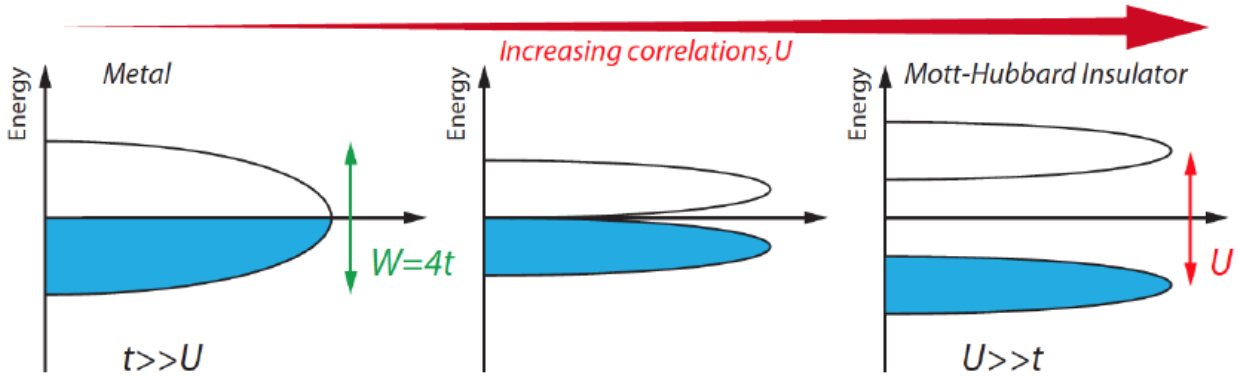

Courtesy D. McMorrow

Strong spin-orbit coupling limit

$$\mathcal{H} = \mathcal{H}(t,U)_{Hubbard} + \lambda \sum_i \mathbf{S}_i \cdot \mathbf{L}_i$$

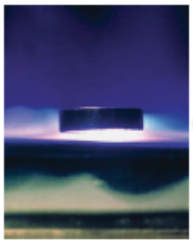

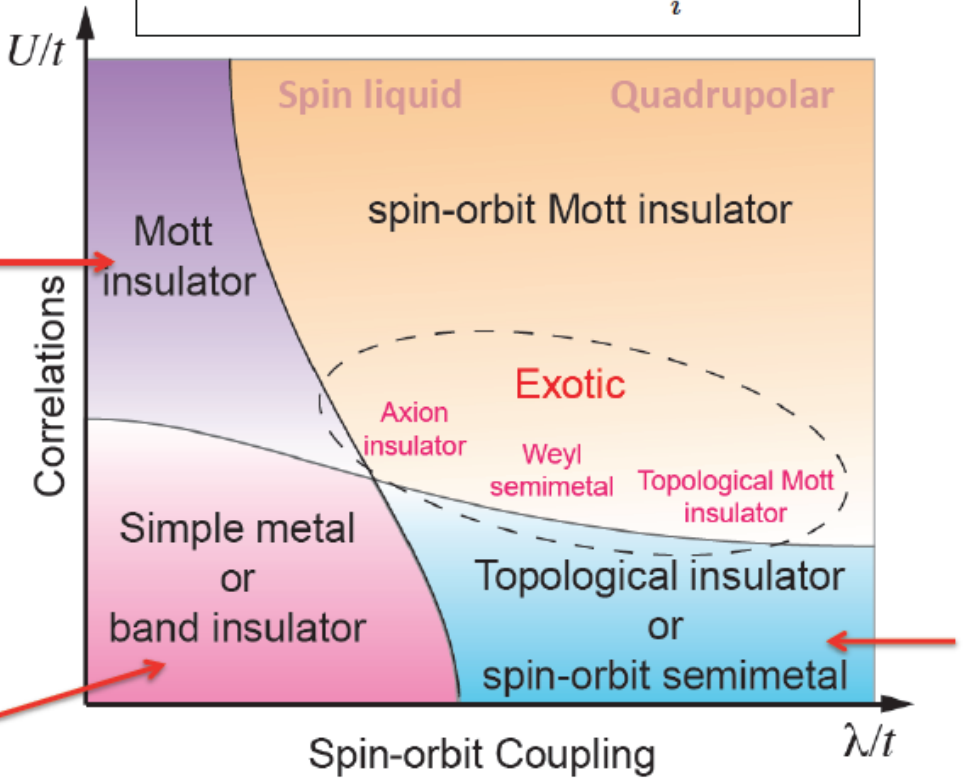

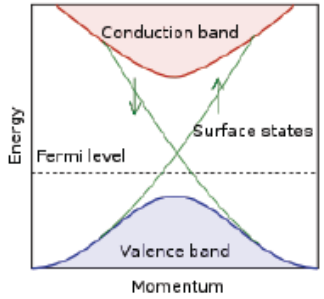

Witczak-Krempa Et al., arXiv:1305.2193

THE J_{eff}=1/2 STATE IN SPIN-ORBIT MOTT-HUBBARD INSULATORS

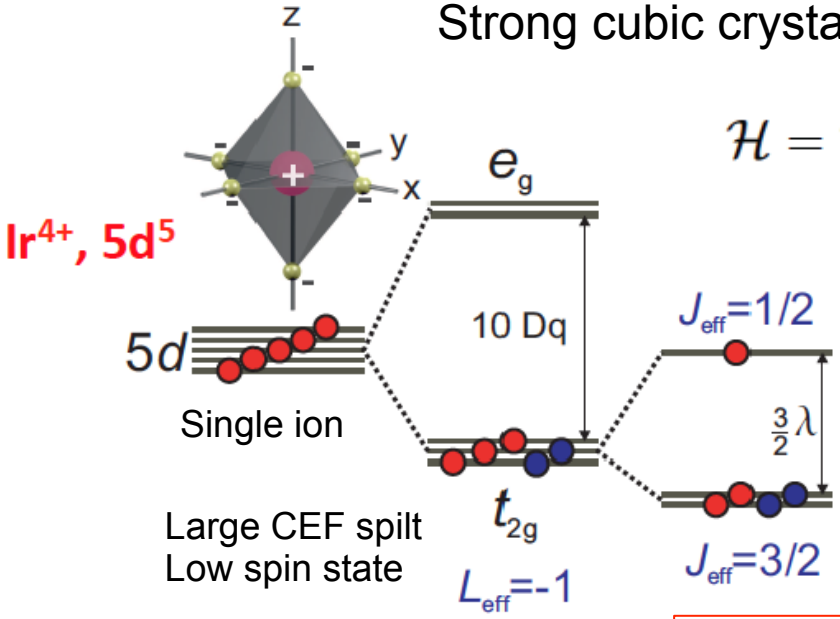

Strong cubic crystal field and spin-orbit coupling limit

$$\mathcal{H} = \mathcal{H}(t,U)_{Hubbard} + \lambda \sum_i \mathbf{S}_i \cdot \mathbf{L}_i$$

Entanglement of spin and orbital moments

$$|j_{\text{eff}} = \frac{1}{2}\rangle_c = \frac{|xy,-\rangle + |yz,+\rangle - i|zx,+\rangle}{\sqrt{3}}$$

Electron band formation and the opening of a Mott gap

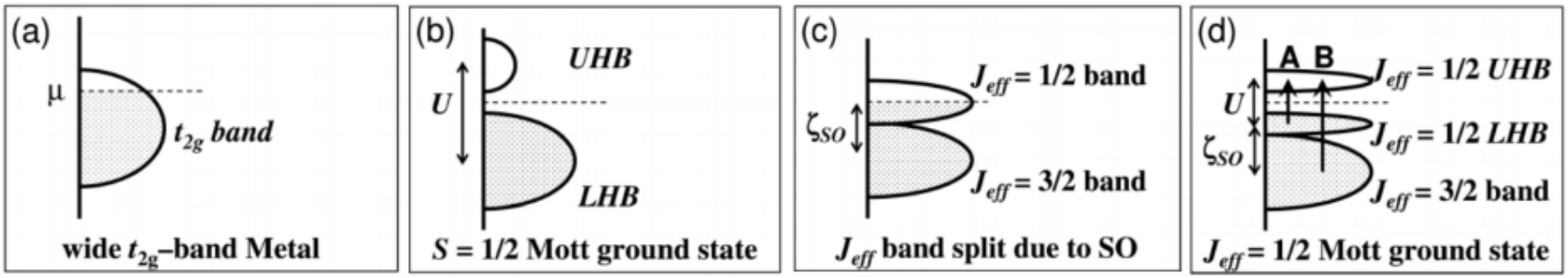

Z-DEPENDENCE OF ENERGY SCALES

Courtesy D. McMorrow

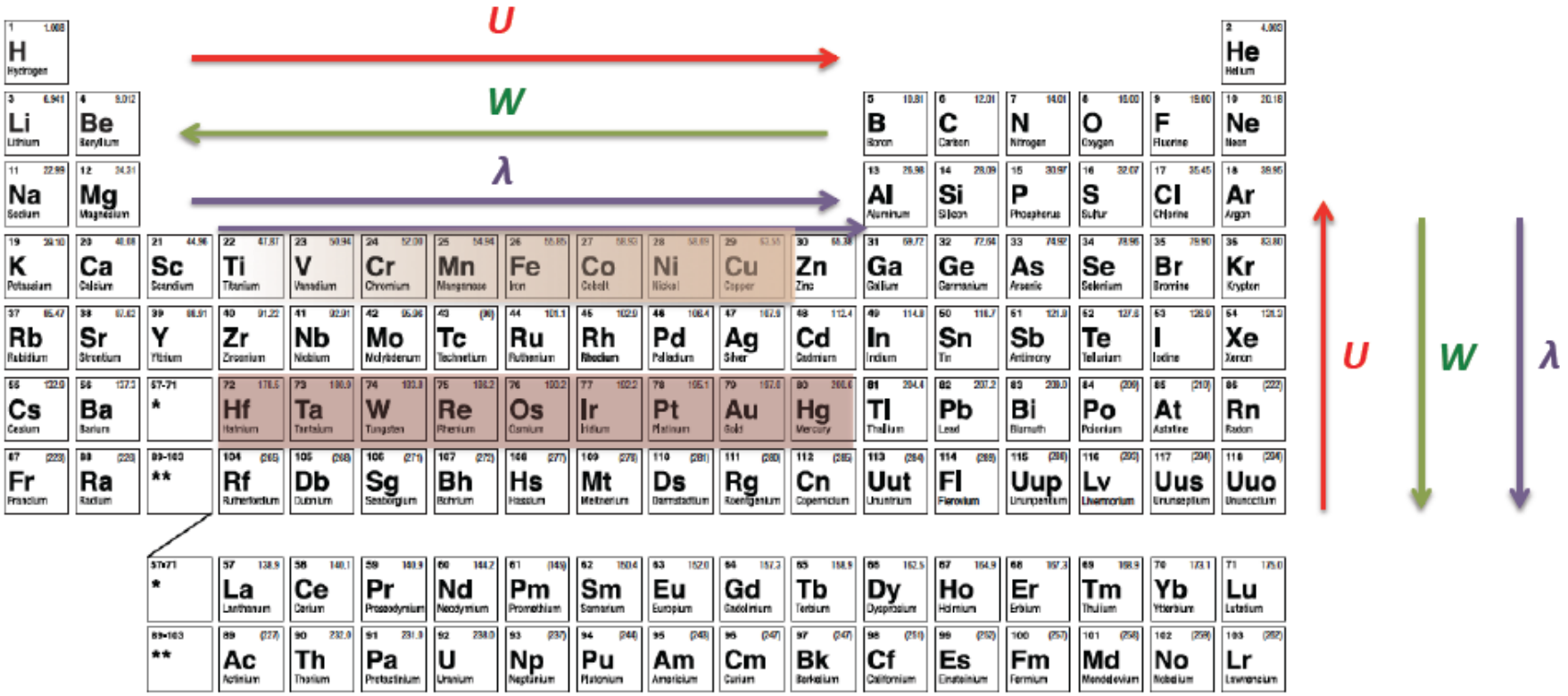

3d Transition metals:

U>>W -> strongly correlated: λ is small

5d Transition metals:

U~W -> metal in absence of spin-orbit coupling: λ is big

U~l -> similar energy scale (1eV) plays a decisive role

Delocalisation imply covalency effects, which may also play an important role

RIXS IN 2D QUANTUM HEISENBERG ANTIFERROMAGNET Sr_2IrO_4

- Strong spin-orbit coupling for Ir^{4+} yields J_{eff}=1/2
- Single magnon dispersion up to 250 meV
- J_{eff} |1/2> → |3/2> excitons at high energy

RIXS at L_3 Ir edge (11.2 keV)
T_N ~ 230 K, k = (½, ½, 0)

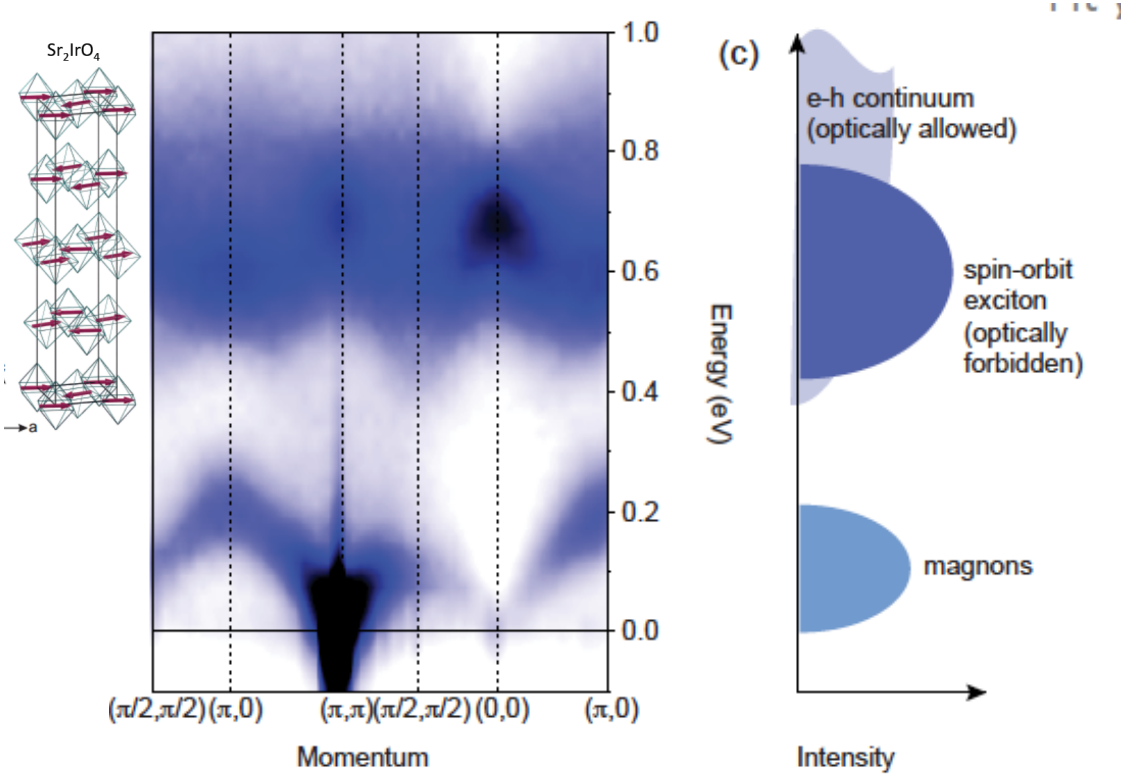

J. Kim et al. PRL 108, 177003 (2012)

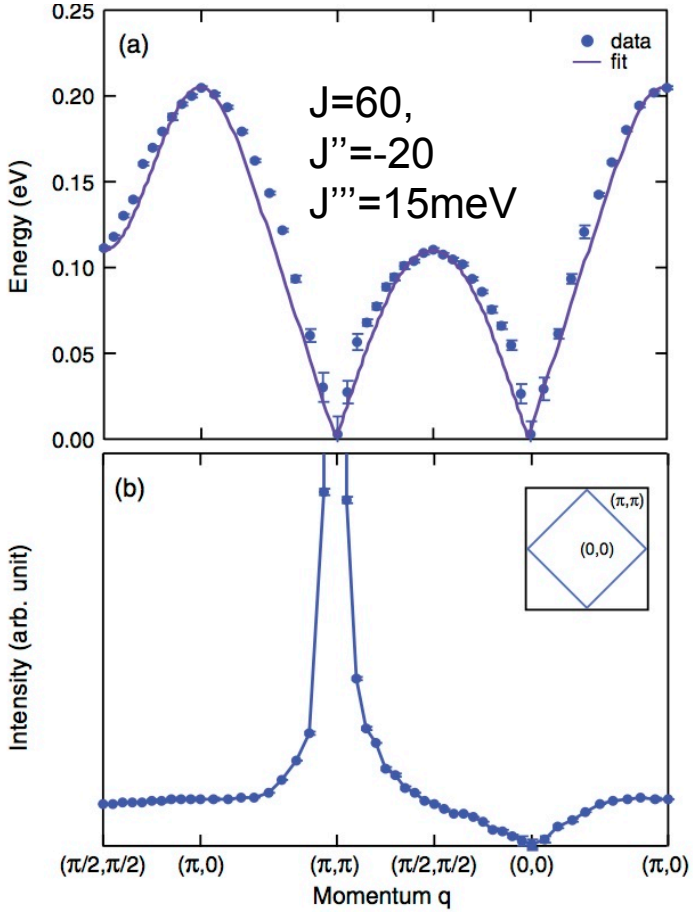

Courtesy D. McMorrow

Neutron and x-ray spectroscopies

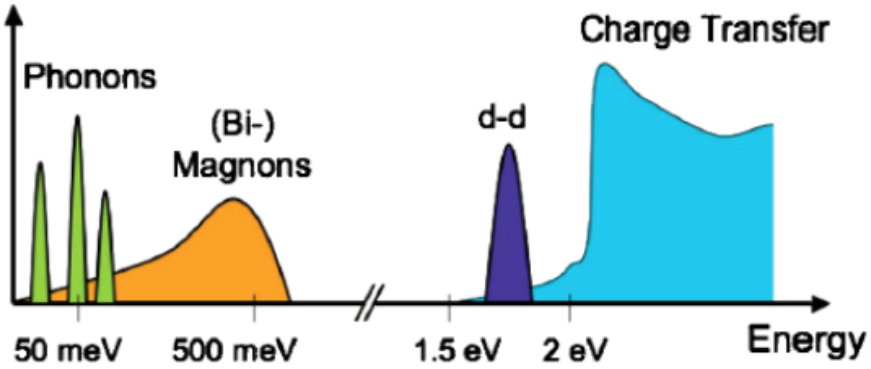

Inelastic Neutron Scattering
2D Mott Insulator La_2CuO_4

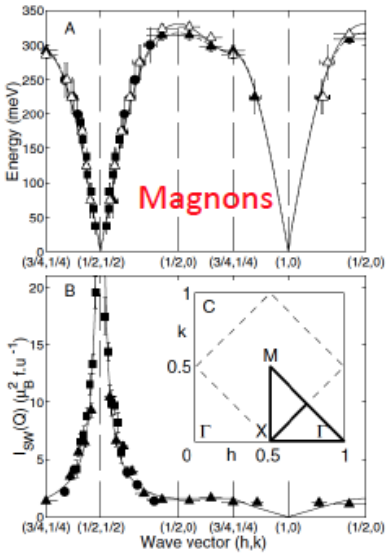

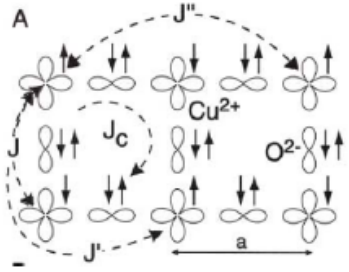

Coldea et al. Phys. Rev. Lett. (2001)

Resonant Inelastic X-ray Scattering
1D Mott Insulator Sr_2CuO_3

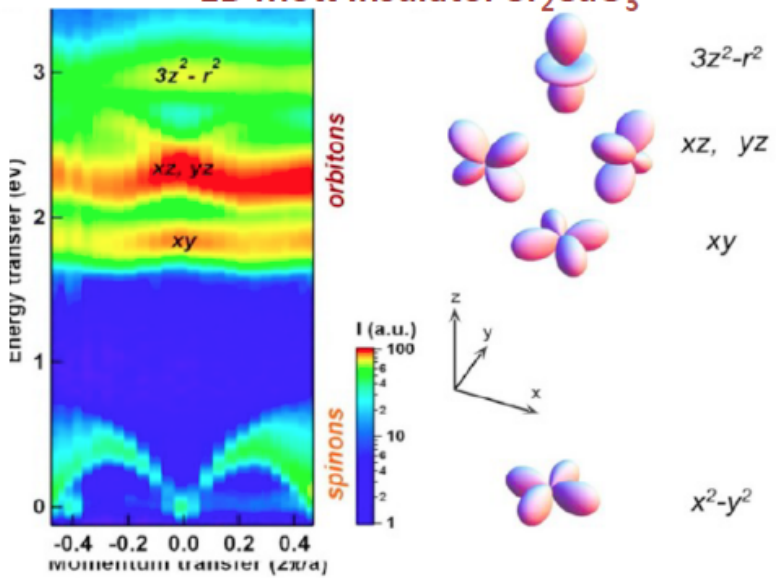

Schlappa et al. Nature (2012)

NEUTRON AND X-RAYS FOR MAGNETISM

Courtesy C. Vettier

Neutrons will remain the main probe to study magnetic structures and magnetic excitations:

- a genuine magnetic probe
- well understood scattering cross section that allows direct comparisons with models
- wide energy range covering the main region of interest
- very good (tuneable) energy resolution
- flexibility of use (providing neutron sources are still available)
- neutron polarisation is a very useful tool

X-rays have made impressive progress in the studies of magnetism:

- X-rays are more ‘electronic’ : they tell us a lot about electronic states
- REXS and RIXS allow to investigate samples (not all materials) in the hard X-ray range
- X-rays couple to order parameters with different symmetries
- a wide variety of ‘parameters’ at hand: polarisation, azimuthal angle, ….
- they require tiny but ‘good’ crystals

GENERAL CONCLUSIONS

Go for neutrons whenever:

- sample material is ‘unknown’ and full magnetic structure has to be determined
- energy scales are below 300 meV
- neutrons accept ‘bad’ crystals
- if crystals are too small, go for powders (inelastic scattering)

Go for X-rays whenever:

- magnetic structure is partially known
- sample material is a ‘good’ crystal (talking about scattering here)
- various order parameters coexist
- adapted edges (large enhancement) are in the hard X-ray range
- fast time-resolved (or very high-pressure) studies are foreseen

BUT

- Exploit both neutrons and X-rays and choose the best method for your own particular case
- Do not use one method if the other one is better!

Thank you for your attention!

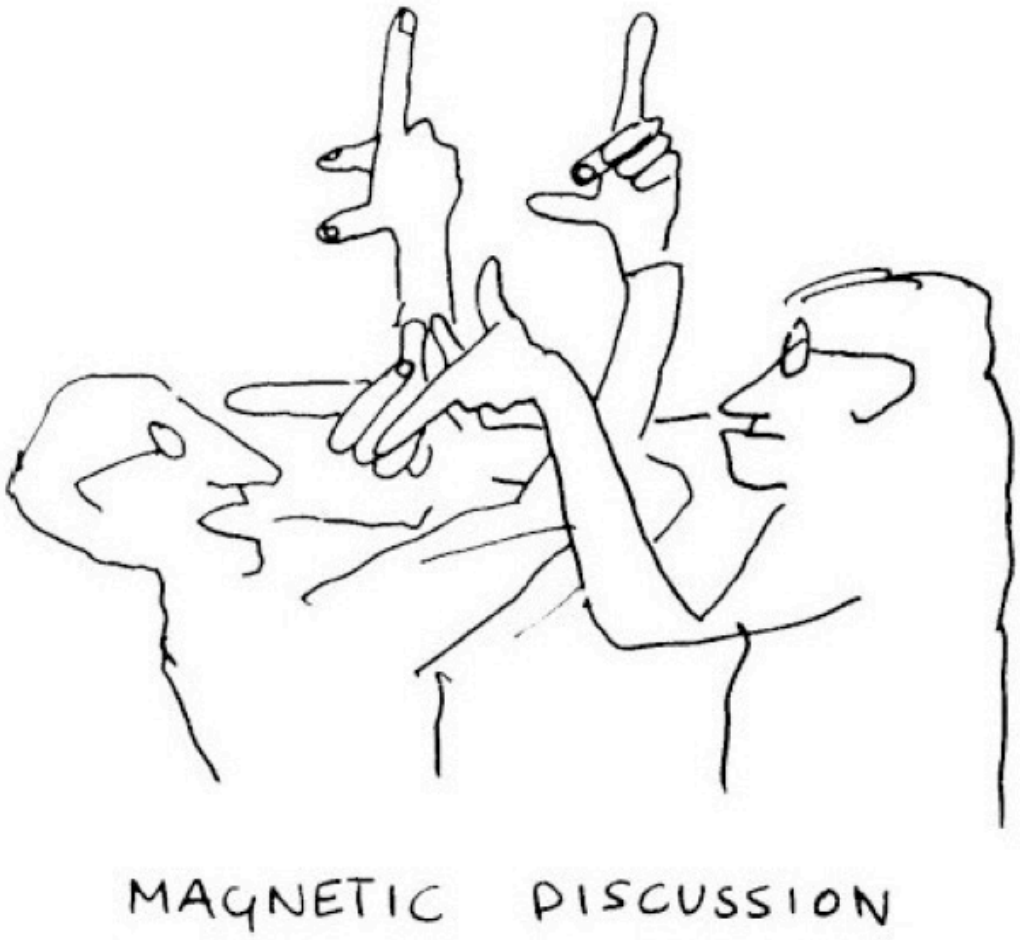

From B. Touschek